

# Marine Geophysical Research

## Seabed mapping in the Pelagie Islands Marine Protected Area (Sicily Channel, southern Mediterranean) using Remote Sensing Object Based Image Analysis (RSOBIA)

--Manuscript Draft--

<b>Manuscript Number:</b>	MARI-D-18-00014R2
<b>Full Title:</b>	Seabed mapping in the Pelagie Islands Marine Protected Area (Sicily Channel, southern Mediterranean) using Remote Sensing Object Based Image Analysis (RSOBIA)
<b>Article Type:</b>	Original Research
<b>Keywords:</b>	Multibeam bathymetry; backscatter; benthoscapes; seabed classification; ground-truth data; Posidonia oceanica; coralligenous habitat.
<b>Corresponding Author:</b>	Sara Innangi Istituto per l'ambiente marino costiero Consiglio Nazionale delle Ricerche ITALY
<b>Corresponding Author Secondary Information:</b>	
<b>Corresponding Author's Institution:</b>	Istituto per l'ambiente marino costiero Consiglio Nazionale delle Ricerche
<b>Corresponding Author's Secondary Institution:</b>	
<b>First Author:</b>	Sara Innangi
<b>First Author Secondary Information:</b>	
<b>Order of Authors:</b>	Sara Innangi Renato Tonielli Claudia Romagnoli Francesca Budillon Gabriella Di Martino Michele Innangi Roberta La Terza Tim Le Bas Claudio Lo Iacono
<b>Order of Authors Secondary Information:</b>	
<b>Funding Information:</b>	
<b>Abstract:</b>	<p>In this paper we present the seabed maps of the shallow-water areas of Lampedusa and Linosa, belonging to the Pelagie Islands Marine Protected Area. Two surveys were carried out ("Lampedusa2015" and "Linosa2016") to collect bathymetric and acoustic backscatter data through the use of a Reson SeaBat 7125 high-resolution multibeam system. Ground-truth data, in the form of grab samples and diver video-observations, were also collected during both surveys. Sediment samples were analyzed for grain size, while video images were analyzed and described revealing the acoustic seabed and other bio-physical characteristics. A map of seabed classification, including sediment types and seagrass distribution, was produced using the tool Remote Sensing Object Based Image Analysis (RSOBIA) by integrating information derived from backscatter data and bathy-morphological features, validated by ground-truth data. This allows to create a first seabed maps (i.e. benthoscape classification), of Lampedusa and Linosa, at scale 1:20 000 and 1: 32 000, respectively, that will be checked and implemented through further surveys. The results point out a very rich and largely variable marine ecosystem on the seabed surrounding the two islands, with</p>

[Click here to view linked References](#)

# Seabed mapping in the Pelagie Islands Marine Protected Area (Sicily Channel, southern Mediterranean) using Remote Sensing Object Based Image Analysis (RSOBIA)

Sara Innangi<sup>1</sup>, Renato Tonielli<sup>1</sup>, Claudia Romagnoli<sup>2</sup>, Francesca Budillon<sup>1</sup>, Gabriella Di Martino<sup>1</sup>, Michele Innangi<sup>3</sup>, Roberta Laterza<sup>5</sup>, Tim Le Bas<sup>4</sup>, Claudio Lo Iacono<sup>4</sup>

<sup>1</sup> Istituto per l'Ambiente Marino Costiero del CNR, Calata Porta di Massa, 80, 80133 Napoli, Italy

<sup>2</sup> Dipartimento di Scienze Biologiche, Geologiche ed Ambientali, Università di Bologna, Piazza di Porta S. Donato 1, 40127 Bologna, Italy

<sup>3</sup> Dipartimento di Scienze e Tecnologie Ambientali, Biologiche e Farmaceutiche, Università degli Studi della Campania "Luigi Vanvitelli", Via Vivaldi 43, 81100 Caserta, Italy

<sup>4</sup> National Oceanography Centre, University of Southampton Waterfront Campus, European Way, Southampton SO14 3ZH, UK

<sup>5</sup> Senior Hydrographic Data Processor / Freelance Geophysicist, 177 Matteo Pagliari 74016 Massafra, Italy

Corresponding Author: [sara.innangi@iamc.cnr.it](mailto:sara.innangi@iamc.cnr.it)

## Abstract

*In this paper we present the seabed maps of the shallow-water areas of Lampedusa and Linosa, belonging to the Pelagie Islands Marine Protected Area. Two surveys were carried out ("Lampedusa2015" and "Linosa2016") to collect bathymetric and acoustic backscatter data through the use of a Reson SeaBat 7125 high-resolution multibeam system. Ground-truth data, in the form of grab samples and diver video-observations, were also collected during both surveys. Sediment samples were analyzed for grain size, while video images were analyzed and described revealing the acoustic seabed and other bio-physical characteristics. A map of seabed classification, including sediment types and seagrass distribution, was produced using the tool Remote Sensing Object Based Image Analysis (RSOBIA) by integrating information derived from backscatter data and bathymorphological features, validated by ground-truth data. This allows to create a first seabed maps (i.e. benthoscape classification), of Lampedusa and Linosa, at scale 1:20 000 and 1: 32 000, respectively, that will be checked and implemented through further surveys. The results point out a very rich and largely variable marine ecosystem on the seabed surrounding the two islands, with the occurrence of priority habitats, and will be of support for a more comprehensive maritime spatial planning of the Marine Protected Area.*

## Keywords

Multibeam bathymetry; backscatter; benthoscapes; seabed classification; ground-truth data; *Posidonia oceanica*; coralligenous habitat.

## 1 **1. Introduction**

2 Marine Protected Areas (MPAs) play a key role in the promotion of the sustainable use of marine  
3 resources and ecological conservation (Agardy 1994). The European Framework and national laws  
4 award protect those particular areas by imposing measures to monitor the environmental status of  
5 such areas (e.g. Jameson et al. 2002; Pomeroy et al. 2005; Guidetti et al. 2008; Pieraccini et al. 2016).  
6 The Pelagie Islands Marine Protected Area (Sicily Channel, southern Mediterranean) is characterized  
7 by different geological features (including sedimentary as well as volcanic substrate) corresponding,  
8 in association with specific biological communities, to a diversity of marine habitats. In this context,  
9 the Pelagie Islands MPA launched a project (Di Martino et al. 2015; Tonielli et al. 2016; Innangi and  
10 Tonielli 2017) to assess the conservation status and map the distribution of *Posidonia oceanica*  
11 meadows (Hemminga and Duarte 2000; Gobert et al. 2006) and coralligenous habitat (Sartoretto  
12 1994; Barbera et al. 2003; Bonacorsi et al. 2012) This is a major issue in the context of biodiversity  
13 conservation in the Mediterranean, as highlighted in the “Action plan for the conservation of the  
14 Coralligenous and other calcareous bio-concretions in the Mediterranean Sea” (Birkett et al. 1998;  
15 UNEP-MAP-RAC 2008). Although these calcareous bio-concretions are considered well represented  
16 in the Mediterranean Sea, in fact, their precise range of distribution is not yet well known (Agnesi  
17 et al. 2009) and information commonly consist of sparse geo-referenced data on species and habitat  
18 occurrences (Martin et al. 2014). For this purpose, multibeam bathymetry and related backscatter  
19 signal are increasingly used to map benthic habitats (or *benthoscapes*, according to Lacharité et al.  
20 2017), with the support of seafloor samples and/or photographs (e.g. Kostylev et al. 2001; Brown et  
21 al. 2011; Micallef et al. 2012; Innangi et al. 2015; Tonielli et al. 2016). In the Mediterranean these  
22 techniques are useful in determining the presence of the seagrass *Posidonia oceanica* (L.) Delile (  
23 e.g. De Falco et al., 2010; Micallef et al., 2012) and coralligenous habitats (e.g. Bonacorsi et al., 2012;  
24 Bracchi et al., 2015, 2017). Indeed, through a qualitative and quantitative analysis of acoustic  
25 backscatter data, MultiBeam Echo Sounder (MBES) systems have been used in the last decades to  
26 infer a number of physical, geological and biological proprieties of the seafloor, such as surface  
27 roughness (e.g. Stewart et al. 1994; Fonseca and Mayer 2007; Fonseca et al. 2009), sediment grain  
28 size (e.g. Collier and Brown 2005; Bentrem et al. 2006; Lo Iacono et al. 2008; Brown and Blondel  
29 2009), substrate type (e.g. Dartnell and Gardner 2004; Karoui et al. 2009), and distribution of  
30 seagrass meadows and other biota (e.g. Innangi et al. 2008, 2015, 2016; De Falco et al. 2010;  
31 Bonacorsi et al. 2012; Micallef et al. 2012; Bracchi et al. 2015, 2017; Tonielli et al. 2016). Moreover,  
32 it has been shown that the variation of backscatter intensity is related to sediment properties (Briggs

1 et al. 2002; Goff et al. 2004; Parnum et al. 2005; Ferrini and Flood 2006; Sutherland et al. 2007). The  
2 aim of this paper is to create seabed maps of the insular shelf of Lampedusa and Linosa through  
3 information obtained from geophysical and ground-truth data. Moreover, we test the capability of  
4 RSOBIA (*Remote Sensing Object Based Image Analysis*; Le Bas, 2016), i.e. an OBIA application  
5 integrated into ESRI's ArcMap GIS, as an objective and quantitative method to interpret geophysical  
6 data with time-savings and simplified procedures. Automated classification systems are becoming  
7 more widely used in seabed mapping due to the need for repeatable, statistically-based and  
8 unbiased procedures supporting the verification of acoustic variability in relation to seabed  
9 properties (Biondo and Bartholomä 2017). For marine benthic habitat mapping, these applications  
10 may allow the identification of homogeneous and discrete areas of the seabed characterized by  
11 different biophysical characteristics, such as bathymetry, occurrence of hard/soft substrates,  
12 sediment types and biological structures (Lacharité et al., 2017). RSOBIA, like eCognition software  
13 made by Trimble (e.g. Lucieer 2008; Diesing et al. 2014; Montereale Gavazzi et al. 2016; Lacharité  
14 et al. 2017; Ierodiaconou et al. 2018), allows to analyze acoustic backscatter mosaic and bathymetric  
15 data characteristics (i.e. depth, roughness and slope) and, through the integration with other data  
16 such as ground-truth information, provides semi-automated acoustic seabed classification of  
17 multibeam images. The produced seabed maps will thus contribute to the mapping of benthic  
18 habitat in shallow water areas around the Pelagie islands and could be of support for a more  
19 comprehensive maritime spatial planning of the Marine Protected Area. Good quality information  
20 on the spatial distribution of vulnerable species and their associated habitats is crucial for successful  
21 conservation measures and critical to decision-makers and managers (Martin et al. 2014).

## 22 **2. Study area**

23 The Pelagian Archipelago (Sicily, Italy) is located in the Sicily Channel (central Mediterranean Sea,  
24 Fig. 1), lying on the African lithosphere, i.e. the Pelagian Block. This was affected by crustal stretching  
25 active in the Neogene-Quaternary, giving rise to an intraplate rift system (Lentini et al., 1995; Civile  
26 et al., 2010 and references herein). The Sicily Channel is an epicontinental sea, with average depth  
27 of less than -400 m, locally interrupted by deep, tectonically-controlled, NW-SE oriented troughs  
28 (Pantelleria, Malta and Linosa grabens; Lanti et al. 1988; Grasso et al. 1991; Civile et al. 2010; Argnani  
29 1990; Fig. 1). Anorogenic (mainly alkaline to peralkaline) volcanism of Neogene-Quaternary age is  
30 developed in correspondence of Pantelleria and Linosa volcanic edifices (Grasso and Pedley 1985;  
31 Calanchi et al. 1989). The Sicily Channel is a high-energy site with a dynamic and highly variable

1 current system that exchanges waters between the Western and Eastern Mediterranean Basins. In  
2 particular, a water mass (about 200 m thick) of Modified Atlantic Mediterranean Water (MAW)  
3 flows eastward, (Fig.1, inset) and, after entering the Sicily Channel, splits into two main branches,  
4 the Atlantic Ionian Stream (AIS) and the Atlantic Tunisia Current (ATC) (Fig. 1; Astraldi et al. 2001;  
5 Poulain et al. 2012). This complex circulation patterns, together with bottom structures such as  
6 seamounts, banks, volcanoes, pockmarks and steep-walled basins, are the main factors responsible  
7 for the biodiversity richness of the Sicily Channel, where healthy deep coral communities find  
8 favorable habitat and several pelagic species such as anchovies, bluefin tuna and fin whales have  
9 spawning and feeding areas (UNEP-MAP-RAC 2015). This study focuses on Lampedusa and Linosa  
10 shallow-water marine area. Lampedusa is the largest island of the Pelagian archipelago, showing a  
11 surface area of 20 Km<sup>2</sup> and a maximum elevation of 133 m above sea level. It is entirely made of  
12 sedimentary rocks (mainly biolites and calcarenites), ranging in age from Late Miocene to Late  
13 Pleistocene (Grasso and Pedley 1988). Linosa Island differs from Lampedusa because it is the  
14 emerging tip of a larger volcanic complex, lying on the western shoulder of the Linosa graben (Fig.1;  
15 Grasso et al., 1991). The island shows a surface area of about 5.4 km<sup>2</sup> and has a maximum elevation  
16 of about 195 m above sea level. Despite their different nature, both islands show, in shallow-water,  
17 the occurrence of insular shelves covered by terraced, submarine depositional bodies. These  
18 represent a common feature on steep and narrow shelves such as on insular, volcanic or  
19 tectonically-controlled margins (Chiocci et al. 2004).

### 20 **3. Methods**

#### 21 *3.1 Acoustic data acquisition and processing*

22 Geophysical data were collected by the Institute for Coastal Marine Environment of the National  
23 Research Council (IAMC-CNR) of Naples (Italy) around Lampedusa and Linosa islands down to 50 m  
24 and to 190 m of depth, respectively (see “MBES lines” in Fig. 2), during two oceanographic surveys,  
25 “Lampedusa 2015” and “Linosa 2016”. Both surveys were performed using a pole-mounted Reson  
26 SeaBat 7125 400 kHz MBES, providing sub-centimetric resolution. The vessels were equipped with  
27 an Omnistar Differential Global Positioning System (DGPS) and an IxSea Octans 3000 gyrocompass  
28 and motion sensor that provided positioning data (with sub-meter accuracy) and attitude data  
29 (0.01° accuracy). A Valeport miniSVS sound velocity probe and a sound velocity profiler were used  
30 to provide the real-time surficial sound speed for the beam steering and the velocity profile required  
31 for the depth computation. The Reson PDS2000 4.1.2.9 version was used for logging and processing

1 MBES bathymetric data: tide data, recorded during acquisition, were applied to all dataset to set up  
2 the real depth before starting the despiking process to generate a final 2.5x2.5 m resolution grid  
3 model. Backscatter data were also collected by MBES systems as snippet data (De Falco et al. 2010;  
4 Innangi et al. 2015). Snippet data processing was carried out using FMGeocoder Toolbox (FMGT) in  
5 Fledermaus 7.6 version (QPS 2016). These data were corrected for receiver gain, transmit power,  
6 transmit pulse width, spherical spreading, attenuation in the water column, area of ensonification,  
7 beam pattern, speckle noise and, finally and most importantly, for angular dependence and local  
8 slope (Mallace 2012; QPS 2016). The final mosaic was exported as a geo-referenced TIFF image with  
9 a 2.5 m pixel size and imaged using a grey scale in which higher backscatter values correspond to  
10 darker areas. A range of signal values spanning from -60 dB to -25 dB was adopted in the maps. The  
11 MBES used for this study was not calibrated to obtain absolute backscatter levels. Consequently,  
12 backscatter data presented are in relative (dB) units and cannot be compared with absolute values  
13 reported in other studies, as in De Falco et al. (2010). However, the backscatter facies have been  
14 locally calibrated with ground-truth information derived from sea-bottom samples and video  
15 images, enabling to infer the nature of the different substrata.

### 16 *3.2 Ground-truth information*

17 During the surveys, sea-bottom samples and video images were collected as ground-truth  
18 information. During the “Lampedusa 2015” survey, due to the boat’s limited dimension, direct  
19 assessment was carried out through video-camera inspections. A GoPro Hero 3 White camera with  
20 1080p resolution, 5 MP photos with 3 fps burst mode with integrated flat lens housing, remotely  
21 controlled, was used. During “Linosa 2016”, both seafloor samples and direct observations were  
22 carried out by using, respectively, a Van Veen grab and a Pollux III R.O.V (Remote Operated  
23 Underwater Vehicle) equipped with two video cameras (high and low resolution). Figure 2 shows  
24 the locations and the coordinate points of the ground-truth data at Lampedusa and Linosa. Seafloor  
25 samples were photographed on deck and their lithological macroscopic features described. Then,  
26 several sub-samples were taken from the homogenized sample and grain-size analyses were  
27 performed in laboratory. The sediments were washed with hydrogen peroxide solution (30% v/v)  
28 and distilled water; the gravel/sand fraction (4-0.125 mm) was analyzed using dry sieving. Grain size  
29 fractions were classified according to the Udden-Wentworth scale (after Pettijohn et al., 1987) and  
30 according to Folk 1980 (Table 1).

### 31 *3.3 RSOBIA*

1 RSOBIA (*Remote Sensing Object Based Image Analysis*) application was used to segment and classify  
2 the seabed of Linosa and Lampedusa with an automatic object-based image analysis (see  
3 <https://conference.noc.ac.uk/product/rsobia-software>). RSOBIA is a new toolbox for ArcMap 10.4  
4 that segments the data layers into a set of polygons. The tool operates by taking multi-layered raster  
5 imagery and segments data into geographic areas with similar statistical properties. Segmentation  
6 and Classification are key techniques for image analysis and this tool gives quick and easy results.  
7 Imagery derivative processing techniques are provided for ease of use but also include texture  
8 analysis techniques such as homogeneity, dissimilarity, contrast and others (Grey Level Co-  
9 occurrence Matrices – GLCMs; <https://conference.noc.ac.uk/product/rsobia-software>). In detail,  
10 segmentation is the process of partitioning a dataset into clusters of contiguous elements that are  
11 similar with respect to a range of selected parameters (Hillman et al. 2017). Each polygon is defined  
12 by K-means clustering and region-growing algorithm, for finding areas and boundaries in the  
13 imagery as well as associated mean and standard deviation of the pixel values within the polygon  
14 (Le Bas 2016; see also Wagstaff et al. 2001; Blaschke 2010; Li et al. 2014). The attribute for each  
15 polygon can be extended with imagery attributes of pixel mean and standard deviation of each data  
16 layer, and wherever ground-truth point data is available. In this way the results from samples, where  
17 available, have been utilized to characterize the class type. The adopted segmentation process has  
18 been taken from RSGIS library of analysis and classification routines (Bunting et al. 2014), specifically  
19 modified to be suitable for the ESRI ArcGIS software under Windows operating system. The RSOBIA  
20 toolbar consists of three sections (Fig. 3), respectively designed for: i) obtaining mathematical  
21 derivatives from a single band imagery, such as slope maps from topography (Fig. 3a); ii) creating  
22 polygonised feature data either by multi-band imagery, or by a combination of single layer grids  
23 making a multi-layered dataset (Fig. 3b); iii) performing the classification and interpretation of  
24 polygonised features (further details on RSOBIA toolbar can be found in Le Bas, 2016). The  
25 segmentation with RSOBIA needs the definition of three main parameters: *Number of Clusters*,  
26 *Minimum Object Size* (the minimum size of any output polygon in terms of pixels, that is the  
27 resolution) and *Layer Weights* (Fig. 3c). In this study, for both islands, we adopted 10 as the number  
28 of clusters, as it was shown to be the optimal number of clusters after several trials, and 20000 as  
29 object size, in relation to the map scale. We decided to run a preliminary test on the segmentation  
30 procedure based on the study by Lacharité et al. (2017), which used backscatter (Fig. 4a) and depth  
31 (Fig. 4b) data layers (BD), from snippet and bathymetry multi-layered raster, where the former was  
32 assigned twice the weight than the latter in order to prioritize substrate composition rather than

1 local variability in depth. Given the geological and morphological differences of the seabed between  
2 the two islands object of this study, we decided to test a second, customized segmentation based  
3 on backscatter, depth, roughness (Fig. 4c) and slope (Fig. 4d) data layers (BDRS), the first one three  
4 times the weight of the others. Such segmentation is intended to also include DTM-derived variables  
5 (such as slope and roughness), however enhancing the role of backscatter signal by increasing its  
6 importance in the segmentation. Hereafter we will refer to these two segmentation approaches as  
7 *BD* and *BDRS*, respectively.

## 8 **4. Results**

### 9 *4.1 Seabed characteristics*

#### 10 *4.1.1 Linosa*

11 The DTM of Linosa shows an articulated morphology, dominated by the occurrence of well-  
12 developed insular shelves down to about 100-120 m depth, all around the SW-S-SE sectors and  
13 offshore the NW of the island (see Fig. ESM1A). The resulting backscatter mosaic of Linosa Island  
14 (Fig. ESM1B) does not show a high variability of the acoustic facies, probably due to the nature of  
15 the volcanic substratum, that tends to oversaturate the acoustic signal, and of the overlying  
16 deposits. In detail, the southern insular shelf (Fig. 5) has a sub-rounded shape and extends for over  
17 1.5 km from the coastline seaward, with an average slope of 3°. It is characterized by two main slope  
18 breaks, at depth of around 45/50 m and 90/100 m (section T'1 in Fig ESM1A), that correspond to  
19 the outer edge of two prograding terraced depositional bodies, lying on the inner part and at the  
20 edge of the insular shelf, respectively (Romagnoli, 2004). In this sector, between -20 and -30 m  
21 depth range, an irregular pattern is evident, both in morphology and in backscatter data. In particular,  
22 the acoustic mosaic shows an intermediate backscatter interrupted by elongated patches of higher  
23 backscatter (ranging in values from -55 to -35dB). This speckled pattern is interpreted as due to  
24 irregular *P. oceanica* meadows (similarly to what was indicated for the Malta offshore by Micallef  
25 et al. 2012). This hypothesis was confirmed by the ROV 6 video images collected at around -33 m  
26 (Fig. 5, sector 1), showing the seagrass organized in dense patches that cover volcanoclastic and  
27 bioclastic coarse sand. Ground-truth data acquired in this sector, below the lower limit of *P.*  
28 *oceanica* (at about 38–39 m depth), confirm that the observed more homogeneous seabed pattern  
29 with high backscatter signal, corresponds to coarse volcanoclastic sand and gravel interspersed with  
30 maërl (see Sample 10 in Fig. 5 and in Table 1). Moving down to 50 m depth (i.e. below the edge of  
31 the shallow-water depositional terrace, see transect T'1 in Fig. ESM1A), more regular acoustic facies

1 occur, with medium-low backscatter (-45/-48 dB), likely corresponding to a finer-grained  
2 sedimentary cover on the seabed. The ROV 7 video images (Fig. 5, sector 2), acquired near a small  
3 morphological high, show the presence of widespread rhodolith and maërl beds (Barbera et al.  
4 2003; UNEP-MAP-RAC 2008; Martin et al. 2014) interspersed with bioclastic coarse sand and gravel.  
5 ROV14, carried out at the end of transect T'1 (Fig. ESM1A) on the outer shelf, in an area  
6 characterized by homogeneous pattern of medium/low backscatter (-45/-50 dB, Fig. ESM1A),  
7 showed particularly well-developed Mediterranean coralligenous assemblages in natural conditions  
8 (Laborel 1961; Ballesteros 2006; UNEP-MAP-RAC 2008; Bonacorsi et al. 2012), hereafter described  
9 according to the video acquisition (i.e. moving upslope from 150 m to 80 depth Fig. 5 sector 3).  
10 Medium to fine bioclastic sand and mud are present on the seabed at -150 m (sample 6 in Fig. 5,  
11 sector 3 and in Table 1); subsequently, along the ROV transect, the volcanic bedrock is covered by  
12 increasing coralligenous concretions (at -135 m, Fig. 5, sector 3). At about 100–85 m depth the  
13 *Lithophyllum stictaeforme* (Areschoud) Hauck and coralligenous assemblages appeared to increase  
14 in size proportionally with decreasing depths (see samples 7 and 8 in Fig. 5 sector 3). At about 83-  
15 80 m depth (Rov14 video frame and sample 9 in Fig. 5, sector 3), a coral community organized in  
16 small banks with sponges, hydrozoans, bryozoans, serpulids, echinoderma, tunicates, and other  
17 organisms was recognized (see also Pérès and Picard 1964; Laborel 1987; Ballesteros 2006). Moving  
18 westwards, in the area offshore the Linosa village, ROV 15 was acquired between 30 and 70 m depth  
19 range (Fig. 6, sector 1). A relatively homogeneous pattern of intermediate backscatter (with slightly  
20 higher values, -45 dB, at shallow depth and lower values, -35 dB, at increasing depth) corresponded,  
21 on ROV images, to a mixture of medium-coarse bioclastic (predominant at -70 m) and volcanoclastic  
22 (predominant at -30 m) sands. In shallow water (-30 m) a few specimens of *P. oceanica* are also  
23 present on the seabed. No grab samples are available for this transect. Most of the submarine  
24 western flank of Linosa shows, down to -80/90 m, a higher backscatter value (about -35 dB)  
25 compared to surrounding areas (see Fig. ESM1B). Sample 3 (Table 1), collected at -53 m on this  
26 acoustic facies is made of volcanoclastic medium sand (Fig. 6, sector 2). More to the north-west,  
27 images from ROV 11 and Sample 5 at about 130 m depth show the occurrence of bioclastic very  
28 coarse sand (Fig. 6, sector 3) with scattered rhodoliths/maërl and, at shallower depth (-80 m),  
29 abundant encrusting organisms on bedrocks (Fig. 6, sector 3). Off the northern coast of Linosa, a  
30 NNW-SSE oriented insular shelf develops for over 1 km far from the island, corresponding to the  
31 Secca di Tramontana shoal (Fig. ESM1A and Fig. 7). It partly corresponds to the remnant of a largely  
32 dismantled eruptive center located to the N of the island (Lanti et al. 1988; Lanzafame et al. 1994).

1 The flanks of Secca di Tramontana appear to be asymmetric, with a steeper eastern side (about 25°  
2 affected by a wide scar corresponding to a canyon head (Romagnoli 2004) and a less steep (5° on  
3 average) terraced western flank (transect T'2 in Fig. ESM1A). On the Secca di Tramontana shoal the  
4 seabed shows high backscatter values at the top (ranging from -35 to -30 dB at around 20-25 m  
5 depth), probably due to the high reflectivity of the bedrock, which by far corresponds to the main  
6 component of the backscatter strength. Two ROV video-inspections were carried out on the western  
7 side of the shoal to determine the *P. oceanica* extension. ROV 1 at 25 m depth and ROV 2 at 28 m  
8 depths showed well-developed and dense *P. oceanica* meadows lying on a rocky substrate (Fig. 7,  
9 sector 1) while, both at lower (-20 m) and higher (-48 m) depth, *P. oceanica* is absent, except for  
10 scattered tufts, while photophilic algae predominate (Fig. 7, sector 1 and sector 2). The NE and E  
11 submarine flanks of Linosa are quite steep (slope between 14 and 25°) and affected by active gullies  
12 and canyon heads also in shallow water, due to the lack of well-developed insular shelf here (except  
13 in the sector SE of the island; Fig. ESM1A). Backscatter in these areas is mainly high, with alternating,  
14 local low-backscatter areas (Fig. ESM1B). Sample 4 was collected in one of the clearer acoustic facies  
15 visible in this sector (about -58 dB; Fig. 8, sector 1), indicating the occurrence of mainly bioclastic  
16 fine sand with a limited volcanic fraction. In the SE sector, the shelf extends with a ENE-WNW  
17 elongated shape for about 1,7 km from the island. On its surface, some erosional remnants can be  
18 observed among which, in particular, two flattened and strongly eroded sub-conical eruptive  
19 centers, each around 160 m in diameter (Fig. ESM1A and Fig. 8, sector 2 and 3). These two  
20 dismantled volcanic cones show concentric summit features (erosional remnants) and are  
21 characterized by intermediate backscatter values (-50 to -45 dB). On the eastern volcanic cone at  
22 about 100 m depth, ROV 4 showed a seabed covered by coralline alga *Lithophyllum stictaeforme*  
23 and other calcareous-coral algae (Fig. 8, sector 2). Moving upslope, from about 95-90 m to 50 m  
24 depth, well-developed rhodolith beds completely cover the underlying substrate made of bioclastic  
25 and volcanoclastic coarse sand (Sample 1 in Fig. 8, sector 2 and Table 1), while at the end of the video  
26 acquisition (depth around 33 m), a rocky substrate, covered with photophilic algae, was observed  
27 on the top of the volcanic cone (corresponding to a speckled, intermediate backscatter pattern; Fig.  
28 8, sector 2). Similarly, ROV 5 surveyed the characteristics of the seabed close to the western cone  
29 and on its top, starting at -88 m (Fig. 8, sector 3). Here the video images showed dense rhodolith  
30 beds as well, decreasing with depth and replaced upslope by mærl beds and coarse volcanoclastic  
31 sands (Sample 2 in Fig. 8, sector 3 and Table 1). In turn, mærl disappears at around -50 m, where a  
32 rocky substrate covered with photophilic algae can be found.

#### 1 4.1.2 Lampedusa

2 The high-resolution DTM of Lampedusa (depth range of 2-50 m, Fig. ESM2A) shows a rugged  
3 seafloor all around the island within the first 20-40 m depth, due to extensive rocky outcrops,  
4 localized talus deposits and relict morphologies on the seabed, as *P. oceanica* meadows on 'matte'  
5 facies (as defined by Francour et al., 2006; see Fig.es ESM2A and B). Locally, vertical scarps 10-20 m  
6 high are present, such as in the eastern and northern shallow-water sectors. As recognizable on  
7 morphological sections (see Fig. ESM2A), the shallow water areas have different characteristics.  
8 Along the northern coast of the island the seabed is steeper ( $3.80^\circ$  on average) (see figure 4 in  
9 Tonielli et al., 2016) and dips down to over -50 m. Conversely, along the southern sector of the  
10 island, the seabed slopes with a gradually decreasing gradient (about  $1.80^\circ$  on average) in the depth  
11 range of 10-50 m. In the SW and SE sectors, in particular, gently-sloping, terraced morphologies  
12 extend from the coast seaward (with average slope of  $1.20^\circ$  to  $0.7^\circ$ , respectively; see bathymetric  
13 transects T1 and T2 in Fig. ESM2A). This setting is due to both the geological structure of the island  
14 (see Grasso and Pedley, 1985) and the occurrence of erosive-depositional features, such as erosive  
15 surfaces and overlying sedimentary bodies. As showed for the island of Linosa, the acoustic  
16 backscatter mosaic is made up by the range of signal values ranged from -60 dB (lighter tones,  
17 corresponding to low backscatter) to -25 dB (dark grey tones, considered as high backscatter). Direct  
18 inspections with GoPro Hero 3, located in selected sites (Fig. 2a and Fig.es ESM2A and B) allowed to  
19 locally calibrate some of the acoustic facies in the southern and eastern submarine areas around  
20 Lampedusa and to better define some specific seabed features. In detail, figure 9 shows the  
21 bathymetry and the acoustic (backscatter) facies of the SW terrace (morphological transect T1 in  
22 Fig. ESM2A). In the deeper, gently-sloping area at about 30/40 m depth, characterized by alternating  
23 low (-55/50 dB) and high (-40 dB) acoustic backscatter, local bathymetric irregularities were  
24 observed on the seabed. These corresponded to a dune field (area of  $0.22 \text{ Km}^2$ ), with NNE-SSW  
25 oriented asymmetric crests, wavelength between 25 and 50 m and a maximum height of about 2 m  
26 (Tonielli et al. 2016). Video 3 was recorded on the dune field, to verify the presence of maërl or  
27 rhodoliths as reported by Di Geronimo and Giaccone 1994 (see also Giardina and De Rubeis 2012).  
28 The ROV images (Fig. 9, sector 1) showed an undulating and irregular seabed covered with soft  
29 sediments, likely composed of medium-fine sand. Given the limited resolution of the images, we  
30 were unable to verify the presence of maërl or rhodoliths on the seabed. Moving upslope on the  
31 SW terrace, video 2 (Fig. 9, sector 2), recorded at a depth ranging between 10 and 38 m, in  
32 correspondence of an irregular seafloor with shortly spaced, v-shaped furrows and with variable

1 backscatter, the presence of *Cymodocea nodosa* (Ucria) Aschers was revealed on a sandy seabed.  
2 Close to the SW edge of the island, video number 1 (Fig. 9, sector 3) allowed to check the nature of  
3 the rugged seabed and the speckled acoustic facies observed in very shallow water, between 5 and  
4 10 m depth. Here the occurrence of very coarse, heterogeneous materials (well-rounded pebbles  
5 and boulders) on poorly sorted gravel is observed, at the foot of the submerged cliff. On the western  
6 flank (Fig. 9, sector 4) the acoustic facies was spotted, presumably indicating an irregular substratum  
7 with coarse-grained sediment (characterized by backscatter values of -30 to -25 dB) covered by *P.*  
8 *oceanica* (corresponding to lower backscatter values of about -40 dB). Due to adverse weather  
9 conditions, it was not possible to acquire video images in this sector, but the occurrence of *Posidonia*  
10 is supported by previous Authors (see Tonielli et al. 2016 and references therein) and the  
11 interpretation of similar acoustic facies (see also Micallef et al. 2012; Truffarelli et al. 2012). *P.*  
12 *oceanica* meadows on 'matte' facies was present, instead, offshore the southern sector of the  
13 island, where backscatter pattern showed circular areas values with a more homogeneous,  
14 intermediate pattern (Fig. 9, sector 5; see Innangi et al. 2015 for 'matte' description). Video 4  
15 allowed to check the lower limit of the *P. oceanica* meadows that here gradually thin out, both in  
16 terms of density of leaves and height, at about 38 m depth on a sandy seafloor (Fig. 9, sector 5).  
17 Offshore the SE part of the island a NNW-SSE oriented, 4-6 m-high scarp delimited the SE terraced  
18 sector westward between 30 and 50 m of depth and corresponded to a morphological step (Fig. 10,  
19 sector 1 and T2 transect in Fig. ESM2A), in agreement with the main structural lineaments  
20 recognized on the island (Grasso and Pedley 1985). The rugged seafloor and irregular acoustic facies  
21 with intermediate backscatter (values around -45 dB) and elongated patches of high backscatter,  
22 characterizing this area down to -30/-40 m, is due to the presence a well-developed *P. oceanica*  
23 meadow, as confirmed by video 7 (Fig. 10, sector 2). In deeper areas, a relatively flat seabed with a  
24 high backscatter pattern occurs. Finally, offshore the eastern flank of Lampedusa, in  
25 correspondence of a large and irregular embayment, the seabed is characterized by large variation  
26 in the backscatter signal, probably due to the occurrence of sedimentary flows down the submarine  
27 flank (Fig. ESM2B). Video 5 (Fig. 10, sector 3) and 6 (Fig. 10, sector 4) were both recorded in this  
28 area: Video 5, from a low-gradient area at depth of 30 m on a medium/high backscatter patch,  
29 documents the absence of any seagrass on the medium-coarse sand covered seabed, while video 6  
30 at around 25 m depth revealed well-developed and dense *P. oceanica* meadows over a rocky bottom  
31 characterized by speckled backscatter pattern.

#### 32 4.2 Results of RSOBIA

1 According to the segmentation approach adopted to analyze the seabed at Linosa through RSOBIA  
2 (section 3.3 and Fig. 4 for derivatives), two different results were obtained for the BD and BDRS  
3 segmentations (Fig. 11a and 11b, respectively). A similar approach was followed to analyze the  
4 Lampedusa data with RSOBIA (see ESM3.1 and ESM3.2). A pairwise comparison of the two adopted  
5 segmentations for a sector offshore Linosa can be seen in figure 12 (and in ESM3.3 for Lampedusa).  
6 It showed that BD (in red) and BDRS (in green) segmentations offer comparable results, although  
7 BD is less sensitive to local facies variations and, at Linosa, it is comparable to a simple contouring  
8 of isobaths (Fig. 11a). Accordingly, it was preferred to apply the BDRS segmentation (see section  
9 3.3). The differences obtained between the two segmentations at Linosa are likely related to the  
10 fact that, given its volcanic nature, it shows a greater morphological variability of the seafloor with  
11 respect to Lampedusa. On the other hand, BD and BDRS segmentations were largely overlapping for  
12 Lampedusa, (even if BDRS appears as more sensitive, see Fig. ESM3.3). This suggests that the use  
13 of BD segmentation is more suitable for regular and smoother seafloor without extensive variation  
14 in roughness and slope (such as observed in the application of Lacharité et al. 2017, on a large shelf  
15 sector offshore Canada), while BDRS slightly outperforms BD in case of larger variability in the  
16 seafloor morphology. Starting from the results of BDRS segmentation and the acquired ground-  
17 truth data, the seabed maps of Linosa and Lampedusa have been proposed.

## 18 4.3 Seabed maps

### 19 4.3.1 Linosa

20 For Linosa, the seabed characteristics appears strongly dependent on the benthic habitat: both ROV  
21 investigations and grab samples showed, in fact, a prevalent and widespread bioclastic sedimentary  
22 cover on the seabed and the occurrence of very well-developed coralligenous habitats, with  
23 abundant rhodoliths and maërl beds. Therefore in order to create the seabed map of Linosa (at scale  
24 1: 20 000), extending the information from ground-truth into areas with similar characteristics, the  
25 results of RSOBIA segmentation (i.e. each majority class of the BDRS classification, Fig. 11b) were  
26 associated with benthoscape classes (*sensu* Lacharité et al. 2017), obtaining the following eight  
27 categories and corresponding characteristics (Fig. 13):

- 28 • *B – Bedrock*: homogeneous pattern of high backscatter, high roughness and variable slope.  
29 Locally the bedrock is colonized by seagrass and/or by photophilic algae (e.g. see Rov1 and  
30 2 in Fig. 7).

- 1 • *VP – Volcaniclastic sand with P. oceanica*: intermediate backscatter interrupted by elongated  
2 patches of high backscatter, intermediate roughness (due to presence of seagrass) and low  
3 slope. The seabed composition is characterized by volcaniclastic coarse sand and gravel  
4 (cobbles and pebbles), with scarce bioclastic sand fraction interspaced with maërl (see Rov8  
5 and sample 10 in Fig. 5, sector 1).
- 6 • *VB – Volcaniclastic and Bioclastic sand*: high backscatter pattern, low roughness and low  
7 slope. Seabed composition characterized by volcaniclastic coarse sand with few bioclastic  
8 sand fraction interspaced with maërl (e.g. see sample 3 in Fig. 6, sector 2).
- 9 • *BV – Bioclastic and Volcaniclastic sand*: homogeneous pattern of high backscatter,  
10 intermediate roughness and high slope. Seabed composition characterized by maërl and  
11 bioclastic coarse sand with fewer volcaniclastic sand fractions (e.g. see ROV11 in Fig. 6,  
12 sector 3).
- 13 • *RM – Rhodolith and Maërl beds*: homogeneous pattern of medium/low backscatter, low  
14 roughness, low slope. The seabed composition is characterized by rhodolith and maërl beds  
15 and bioclastic coarse/medium sand (e.g. see ROV7 in Fig. 5, sector 2 and ROV4 in Fig. 8,  
16 sector 2).
- 17 • *RML – Rhodolith, Maërl and Lythophyllum beds*: homogeneous pattern of medium/low  
18 backscatter, low roughness, low slope. The seabed composition is characterized by rhodolith  
19 maërl and *Lythophyllum* beds that cover bioclastic medium/fine sand (e.g. see Rov14 in Fig.  
20 5, sector 3 and Rov4 in Fig. 8, sector 2).
- 21 • *MB – Mäerl and/or Bioclastic fine sand*: homogeneous pattern of low backscatter,  
22 intermediate roughness, high slope. The seabed composition is characterized by maërl and  
23 bioclastic fine sand (e.g. see Rov14 in Fig. 5, sector 3).
- 24 • *Bfs – Bioclastic fine sand*: homogeneous pattern of low backscatter, intermediate roughness,  
25 high slope. The seabed composition is mostly characterized by bioclastic fine sand (see  
26 sample 4 in Fig. 8, sector 2).

27 Moreover, since *Posidonia oceanica* on rock is not recognizable in the segmentation procedures,  
28 but only through the video images (ROV1 and 2 in Fig. 7), further information on benthic habitat  
29 distribution (seagrasses) were manually added as overprinted symbols (*Posidonia oceanica* on rock).  
30 To make the map more consistent, the same was done for the *Posidonia oceanica* on sand even if  
31 this had been recognized in the segmentation (VP). Overall, it can be noted that the first facies of  
32 the benthoscape classification (“Bedrock” in Fig. 13) is common in the NW (“Secca di Tramontana”)

1 and SE shallow-water areas, in correspondence of widely-eroded secondary volcanic edifices on the  
2 insular shelf, and in coastal areas around most of the island, as the prosecution of lava flows in  
3 shallow water. Volcaniclastic sand is abundant along the western shelf, where it is produced by  
4 erosion of tuff rings in the coastal area and reworked in submerged depositional terraces and is  
5 mixed with a bioclastic fraction. This fraction becomes more and more abundant downslope (below  
6 about 50 m depth) and showed scattered rhodoliths and lower grain size with increasing depth.  
7 Conversely, *P. oceanica* meadows on coarse sand are abundant on the inner insular shelf (first 30 m  
8 depth) all along the S flank of the island, above the thick and laterally continuous depositional  
9 terrace, while the frontal scarp of the terrace is covered by volcaniclastic and bioclastic coarse sand.  
10 Facies dominated by calcareous biogenic concretions (Rhodoliths and mäerl) are widespread on the  
11 outer shelf areas (to the SW-S-SE and NW of the island), from about 60 m to about 100 m of depth,  
12 passing to bioclastic fine sand (with associated mäerl) below that depth. The proposed benthoscape  
13 classification is still preliminary because it is based on a first integration of available data. Further  
14 ground-truth data are necessary to better characterize some acoustic facies not extensively sampled  
15 in this first survey, and related ecological systems.

#### 16 4.3.2 Lampedusa

17 In order to create a seabed map for Lampedusa (at scale 1: 32 000), the interpretation of the RSOBIA  
18 shape file focused on BDRS majority classes locally checked through video inspections. Because no  
19 grab sampling is available here, the seabed was, in fact, mainly classified on the basis of its acoustic  
20 facies pattern (i.e. fine sediments exhibiting low backscatter, and coarse sediments corresponding  
21 to high backscatter) and the results of RSOBIA segmentation (majority classes of the BDRS  
22 classification, see section 3.3). So, eight main categories have been described and interpreted with  
23 respect to backscatter, roughness and slope characteristics to produce a preliminary benthoscape  
24 classification of Lampedusa (Fig.14):

- 25 • *A – Speckled pattern of medium backscatter*: interrupted by homogeneous pattern of high  
26 backscatter. It is characterized by high roughness and intermediate slope. The substrate is  
27 mostly composed of bedrock and gravel (Video 1 of Fig. 9, sector 3), but in some sectors  
28 includes patches of *P. oceanica* (Fig. 9, sector 4).
- 29 • *B - Homogeneous pattern of high backscatter*: characterized by low roughness and low slope.  
30 It presumably represents a substratum with coarse-grained sediment.

- 1 • *C - Homogeneous pattern of medium/high backscatter*: low roughness and variable slope. It  
2 presumably represents a substratum with coarse/medium sand, generally without any  
3 evidence of seagrasses (Video 5 of Fig. 10, sector3).
- 4 • *D – Speckled pattern of intermediate backscatter*: interrupted by circular and/or elongated  
5 pattern of high backscatter, intermediate roughness and slope. This class include *Posidonia*  
6 *oceanica* meadows ‘on matte’ (see ESM2 and Fig. 9, sector 5) with holes at which are almost  
7 always filled with coarse sand. The kind of sediment below the seagrass cannot be  
8 constrained without any grab sampling.
- 9 • *E - Speckled pattern of low backscatter*: interrupted by circular and/or elongated pattern of  
10 high backscatter, intermediate roughness and low slope. This class include dense *Posidonia*  
11 *oceanica* meadows interspaced with coarse sand (Fig. 10, sector 1 and video 7 of sector2).  
12 An exception to this is witnessed by Video 2 of figure 9 which showed a sandy seabed  
13 covered by *Cymodocea nodosa*. Future samples will allow to better define the type of  
14 sediment.
- 15 • *F - Speckled pattern of medium/low backscatter*: intermediate/low roughness and slope. This  
16 acoustic facies is the most difficult to classify because it includes both areas with rock and  
17 *Posidonia oceanica* (Video 6 of Fig. 10, sector 4), and the sector to the south of the island  
18 where the lower limit of the *P. oceanica* meadows occurs. *Posidonia* on ‘matte’ here  
19 gradually thins out, both in density of leaves and height (Video 4 of Fig. 9, sector 5). Finally,  
20 it includes the dune sector (Video 3 of Fig. 9, sector 1), likely composed of medium-fine sand.
- 21 • *G - Homogeneous pattern of low backscatter*: low roughness and slope. It likely represents a  
22 substratum with fine grained sediment, without any evidence of seagrasses. This class also  
23 encloses the dune field sector (Video 3 of Fig. 9, sector 1)
- 24 • *H - Homogeneous pattern of very low backscatter*: (very high absorption), low roughness and  
25 slope. It presumably represents a substratum with very fine grained sediment and silt, but  
26 in some cases it includes sectors previously classified by Tonielli et al. 2016 as *Posidonia*  
27 *oceanica* in patches.

28 From interpretations given in section 4.1.2 and map of Fig. 14 it appears that the shallow-water  
29 areas in most of the coastal strip, in particular along the W and NE flanks of the island are  
30 characterized by bedrock covered with very coarse and heterogeneous sediments. A sandy seabed  
31 (from coarse-medium size) was present at very shallow depth along the S flank of the island and, in  
32 general, at increasing depth, gradual shifting to finer-size sand. Again, further information on

1 benthic habitat distribution (seagrasses) have been manually added as overprint layers, consistent  
2 with video inspections (Fig. 14):

- 3 • *Posidonia oceanica* meadows
- 4 • *Posidonia oceanica* to be verified (this area falls under “*Posidonia oceanica* in patch”  
5 according the classification of Tonielli et al. 2016)
- 6 • *Cymodocea nodosa*

7

## 8 **5. Discussion**

9 This paper merges together geomorphological, sedimentological and habitat observations at the  
10 Pelagic Islands of Lampedusa and Linosa, resulting in an integrated, multipurpose seabed mapping.  
11 To this aim we applied the RSOBIA methodology and tested it: 1) on different geological substrata  
12 (volcanic and sedimentary), 2) on very heterogeneous lithological and morpho-sedimentary  
13 conditions (flat or gentle-sloping sea bed, articulated seabed with scarps, volcanic outcrops or loose  
14 sediment, erosive or depositional features) and 3) over a differently-colonized seafloor. In  
15 particular, we found that among the resulting output (shape files) of RSOBIA, the BDRS  
16 segmentation is the most suitable to build the final benthoscape map. We did not adopt a manual  
17 re-classification based on uncertainties in membership values to individual classes – especially at  
18 the boundaries between coverages – as carried out by Lacharité et al (2017). However, it is  
19 important to keep in mind the role of the operator, that remains crucial for the recognition of some  
20 specific acoustic facies, and the need of abundant ground-truth data to characterize acoustic facies  
21 and to support interpretations. As an example of this, at Linosa, the high density of coralligenous  
22 habitat (i.e. maërl, rhodoliths and *Lhytophyllum*) causes a saturation of the backscatter signal to  
23 intermediate values, making the seabed classification difficult through the sole use of acoustic  
24 mosaic. In similar cases, such as at Palinuro Seamount (central Mediterranean; Innangi et al., 2016),  
25 or western Sardinia (De Falco et al., 2010) and northern Tyrrhenian sector of Basilicata (Innangi et  
26 al 2015) the presence of *P. oceanica* meadows (or other biogenic components) on the seabed tends  
27 to reduce the value of backscatter strength, showing an increase in absorption and giving rise to a  
28 possible mismatch between the acoustic facies of medium and/or coarse sands. Thus, the  
29 integration of ground-truth data and the manual processing is required for adequate interpretation  
30 of the acoustic pattern derived from the RSOBIA output. In the southern shallow-water sector of  
31 Linosa, for instance, where the low seabed slope and superficial currents allow a luxuriant growth

1 of coralline environment, BDRS segmentation appears more dependent on bathymetric changes  
2 than on backscatter variations and it underestimates the variability in the benthic habitat. Indeed,  
3 by ROV video images it can be observed that the distribution of *Lhytophyllum* is present here in a  
4 range of depths varying between 100 and 85 meters, while rhodolith beds seem to find their ideal  
5 environment between 60 and 90 meters. The distribution of maërl (composed of spheroidal,  
6 discoidal and ellipsoidal shape branched classes, Peña and Bárbara 2009) is also widely common  
7 around the island. The only well-distinguished facies according to both bathymetry and backscatter  
8 data (well recognized also by BDRS segmentation as majority class 2, Fig. 11b) is the *Posidonia*  
9 *oceanica* meadow on the southern part of the island (depth between -20 m to -36 m) lying on a  
10 coarse-sand substrate (characterized by high backscatter, i.e. darker area on the acoustic mosaic).  
11 The occurrence of *Posidonia oceanica* on rock, on the other hand is not distinguishable without  
12 direct observation, unless it is very dense, both in Linosa and in Lampedusa. Furthermore, where  
13 volcaniclastic sands prevail over bioclastic sands and maërl, the backscatter signal is overbearing in  
14 the BDRS segmentation (i.e. majority class 6, Fig. 11b), as it occurs for fine sand without maërl (i.e.  
15 majority 1, Fig. 11b). At Lampedusa, in absence of grain-size and lithological information, the BDRS  
16 segmentation allowed a preliminary mapping of the seabed typologies, based on morpho-acoustic  
17 data, and will need to be implemented with further investigations. The map obtained through the  
18 object-based method was then integrated with indications of the *P. oceanica* meadows extension,  
19 obtained through video image analysis and previous interpretation of the morpho-acoustic data  
20 (according to Tonielli et al. 2016). To conclude, the combination of RSOBIA segmentation, ground-  
21 truth data and manual processing provide a suitable approach for seabed mapping and for a better  
22 understanding of the fine-scale distribution of benthic habitats. This approach should be supported  
23 by further investigations and sampling of the Pelagie Islands, in order to have more robust  
24 interpretations.

## 25 **6. Conclusions**

26 The surveys carried out around the Pelagie islands revealed a very rich ecosystem, both for the  
27 development of *P. oceanica* and for the presence of coralligenous habitats, confirming what had  
28 been previously proposed by predictive modeling for this area (Martin et al. 2014). In particular, the  
29 morphological setting of Lampedusa, with less steep submarine flanks than Linosa and with a  
30 sedimentary substratum, favors the development of *P. oceanica* meadows. The volcanic seabed at  
31 Linosa, on the other hand, proved to be more suitable for coralligenous environments, characterized

1 by pristine coralligenous habitats that need to be preserved. The reasons for such a highly  
2 productive environment around this island may be several, e.g. the presence of upwelling currents,  
3 or its volcanic nature rich in nutrients, or the low human impact that still prevails here. Our first  
4 seabed mapping supports the enlargement of the Marine Protected Area of Linosa, including the  
5 coralligenous habitat identified on this island and that represents a unique heritage for the  
6 Mediterranean Sea. In conclusion on the seabed of Linosa and Lampedusa three important  
7 ecosystems have been identified (i.e. *Posidonia oceanica*, coralligenous assemblages and mærl).  
8 These area have been recognized as VMEs (Vulnerable Marine Ecosystems) by the EU and other  
9 official environmental commissions (<http://www.fao.org/in-action/vulnerable-marine-ecosystems/en/>; e.g. Francour et al. 2006; Bensch et al. 2009; OCEANA 2009; Bernal 2016). The  
10 seabed classification and the recognition of its priority habitats are basic elements for a proper  
11 management of this Marine Protected Area (e.g. Ehrhold et al., 2006; Bracchi et al., 2015; Le Bas  
12 and Huvenne, 2009; Micallef et al., 2012). Accordingly, as can be seen on the maps, a good extension  
13 of *Posidonia oceanica* (both for Linosa the for Lampedusa) and a rich coralligenous environment (for  
14 Linosa) has been found out the boundaries of the MPA. Thus, our first seabed mapping supports the  
15 enlargement of the Marine Protected Area of Linosa, and suggests the possibility that these  
16 boundaries should be modified, both as extension and as level of protection. The capability to  
17 classify the seabed in an automated or semi-automated manner could guarantee the objectivity and  
18 repeatability of the application over time (e.g. Lucieer 2008; Lucieer and Lamarche 2011; Huang et  
19 al. 2014; Ismail et al. 2015; Lacharité et al. 2017). The use of RSOBIA (integrated by  
20 geomorphological, sedimentological and habitat observations) proved to be a sound method for  
21 this purpose, allowing an initial seabed classification regardless of the availability of grain size  
22 information (as at Lampedusa) or of the clarity of the acoustic facies (as at Linosa).  
23

## 24 **Acknowledgements**

25 We thank Simone D'Ippolito, the captain of the M/B 'Risal', for the help and continuous support  
26 during all the operations of data acquisition.

27 Thanks to the crew of the R/V 'Minerva Uno', for all the support during board and research  
28 operations.

29 The authors wish to thank Sergio Monteleone and Patricia Scaflani for their comments to the first  
30 draft of the manuscript.

## 31 **Funding**

1 This study benefited from contribution of the project “Implementation of research activity and  
2 monitoring around Pelagie Islands Marine Protected Area”, within the project “CAmBiA – Contabilità  
3 Ambientale e Bilancio Ambientale” funded by the Ministry of the Environment and Protection of  
4 Land and Sea (MATTM – Ministero dell’Ambiente e della Tutela del Territorio e del Mare), directive  
5 n° 5135 of march 2015.

6 This study also benefited from the contribution of the RITMARE Flagship Project, funded by Ministry  
7 of Education, University and Research (MIUR – Ministero dell’Istruzione dell’Università e della  
8 Ricerca) [NRP 2011-2013].

## 9 Tables

10 **Table 1** Sediment classification according to Folk (1980) and Wentworth (1987). Left below: histograms of  
11 weight percentage of Wentworth size class. Right below: Folk’s ternary diagram.

## 12 Captions

13 **Fig. 1** Location Map of Lampedusa and Linosa islands in the Sicily Channel (Central Mediterranean Sea, Italy).  
14 Bathymetry are taken from EMODnet portal (<http://www.emodnet-bathymetry.eu/data-products>); the  
15 Pantelleria graben (PG), the Malta graben (MG), and the Linosa graben (LG) are the principal tectonic  
16 depressions of the Sicily Channel. The Atlantic Ionian Stream (AIS) and the Atlantic Tunisia Current (ATC)  
17 (Astraldi et al. 2001; Poulain et al. 2012) are shown (The MAW flows are shown in inset).

18 **Fig. 2** a) MBES navigation lines of the survey “Lampedusa 2015” and positions of collected underwater video  
19 inspections; b) MBES navigation lines, positions of collected ROV inspections and grab samples of the survey  
20 “Linosa 2016”.

21 **Fig. 3** RSOBIA toolbar showing both the derivatives a) and the segmentation b) sub-menu. In c) is shown the  
22 Segmentation window; during the standard segmentation process each layer is given equal weighting  
23 regardless of the differing units used on each layer. The user can provide individual layer weights if, for  
24 example, one layer is deemed to provide more important or better imagery. The derivatives functions are  
25 standard grid manipulation techniques; in this study we used slope and roughness functions; the first  
26 calculates the maximum slope (in any direction) in degrees and values created are real numbers between 0.0  
27 and 90.0 but values of -1.0 is used for areas of no data. This function differs from a shaded relief which is a  
28 slope derivative from particular direction. For roughness, the function calculates the variations in bathymetry  
29 datasets within a neighborhood. This technique combines the variability of slope and aspect in a sampled  
30 area, similarly to the “Benthic Terrain Modeler” developed by Shaun Wallbridge (Wright et al. 2012; Le Bas  
31 2016).

32 **Fig. 4** Raster images used to analyze the Linosa seabed with RSOBIA. a) Snippet mosaic (backscatter), with  
33 brightness values are indicated (low value corresponding to high backscatter and low absorption); b) DTM  
34 image (in meters); c) the surface roughness (in dimensionless value) derived trough RSOBIA; d) the slope  
35 image (in degree) derived trough RSOBIA.

36 **Fig. 5** Bathymetry a) and backscatter b) 3D visualization of the southern part of Linosa. Follow shaded relief,  
37 backscatter imagery, ROV video frame, samples’ photos, description of physical parameters and seabed  
38 composition of three sector investigated in this area of Linosa. See the text for details.

39 **Fig. 6** Bathymetry a) and backscatter b) 3D visualization of the western part of Linosa. In the columns below,  
40 shaded relief images from DTM, backscatter imagery, ROV video frame (where available), samples’ photos  
41 (where available), description of physical parameters and seabed composition of three investigated sector  
42 are reported. See the text for details.

1 **Fig. 7** Bathymetry a) and backscatter b) 3D visualization of the northern part of Linosa. In the columns below,  
2 shaded relief from DTM, backscatter imagery, ROV video frame, description of physical parameters and  
3 seabed composition of two investigated sectors of Linosa are reported. See the text for details.

4 **Fig. 8** Bathymetry a) and Backscatter b) 3D visualization of the eastern part of Linosa. In the columns below,  
5 shaded relief from DTM, backscatter imagery, ROV video frame (where available), samples' photos (where  
6 available), description of physical parameters and seabed composition of three investigated sectors of Linosa  
7 are reported. See the text for details.

8 **Fig. 9** Bathymetry a) and Backscatter b) 3D visualization of the western part of Lampedusa. In the columns  
9 below, shaded relief from DTM, backscatter imagery, GoPro video frame (where available), description of  
10 physical parameters and seabed composition of five investigated sectors of Lampedusa are reported. See the  
11 text for details.

12 **Fig. 10** Bathymetry a) and Backscatter b) 3D visualization of the sud-estern part of Lampedusa. In the columns  
13 below, shaded relief from DTM, backscatter imagery, GoPro video frame (where available), description of  
14 physical parameters and seabed composition of four investigated sectors of Lampedusa are reported. See  
15 the text for details.

16 **Fig. 11** RSOBIA segmentation results: a) from BD segmentation; b) from BDRS segmentation and related  
17 Majority class.

18 **Fig. 12** Pairwise comparison of the two adopted segmentations for a sector of Linosa. BD and BDRS  
19 segmentations offers comparable results, though BD less sensitive lo local facies variations. Furthermore, the  
20 BD segmentation is to comparable to a simple contouring of isobaths.

21 **Fig. 13** Benthoscape classification of Linosa Island obtained with the interpretation of RSOBIA-BDRS  
22 segmentation; Seagrasses on rock and on sand have been added manually as over printed symbols. Also the  
23 areas boundaries of the MPA of Linosa were added in map, where the level of protection decrease from area  
24 A to area C (see <http://www.minambiente.it/pagina/area-marina-protetta-isole-pelagie>).

25 **Fig. 14** Preliminary benthoscape classification of Lampedusa Island obtained with the interpretation of  
26 RSOBIA-BDRS segmentation. Seagrasses have been added manually as over printed symbols. Also the areas  
27 boundaries of the MPA of Lampedusa were added in map.

28

## 29 **Description Electronic Supplementary Material**

30 **ESM1** A) High resolution DTM of Linosa island and shallow water offshore (2.5X2.5 m pixel resolution) with  
31 5 m contouring. The location of bathymetric transects T'1 and T'2 is indicated, as well as ground-truth  
32 points (Rov and grab samples position). B) High resolution snippet mosaic of Linosa island and shallow  
33 water offshore (2.5x2.5 m pixel resolution) with 5 m contouring.

34 **ESM2** A) High resolution DTM of Lampedusa island and shallow water offshore (2.5X2.5 m pixel resolution)  
35 with 5 m contouring. The location of bathymetric transects T1 and T2 is indicated, as well as video points  
36 position. B) High resolution snippet mosaic of Lampedusa island and shallow water offshore (2.5x2.5 m  
37 pixel resolution) with 5 m contouring.

38 **ESM3 1** Raster images used to analyze the Lampedusa seabed with RSOBIA. a) Snippet mosaic  
39 (backscatter), where the brightness values are given (low value corresponding to high backscatter and low  
40 absorption); b) DTM image (in meters); c) the surface roughness (in dimensionless value) derived trough  
41 RSOBIA; d) the slope image (in degree) derived trough RSOBIA. **2** RSOBIA segmentation results: a) shows  
42 the BD segmentation; b) shows the BDRS segmentation. The maps show the majority, the most common

1 class of all pixels in polygon. This is the main class for interpretation. **3** Pairwise comparison of the two  
2 segmentations for a sector of Lampedusa. The BDRS segmentation shows a better recognition of the  
3 acoustic facies boundaries compared to BD segmentation. For this reason, it was decided to adopt the  
4 BDRS segmentation for the interpretation.

5

6

## 7 **References**

- 8 Agardy MT (1994) Advances in marine conservation: the role of marine protected areas. *Trends Ecol Evol*  
9 9:267–70. doi: 10.1016/0169-5347(94)90297-6
- 10 Agnesi S, Annunziatellis A, Casese ML, et al (2009) Analysis on the coralligenous assemblages in the  
11 Mediterranean Sea: a review of the current state of knowledge in support of future investigations. In:  
12 Proceedings of the 1st Mediterranean symposium on the conservation of the coralligenous and other  
13 calcareous bio-concretions. C. Pergent-Martini & M. Bricchet (Eds). UNEP-MAP RAC/SPA (Tabarka, 15-  
14 16 January 2009). Tunis, RAC/SPA publication
- 15 Argnani A (1990) The strait of sicily rift zone: Foreland deformation related to the evolution of a back-arc  
16 basin. *J Geodyn* 12:311–331. doi: 10.1016/0264-3707(90)90028-S
- 17 Astraldi M, Gasparini GP, Gervasio L, Salusti E (2001) Dense Water Dynamics along the Strait of Sicily  
18 (Mediterranean Sea). *J Phys Oceanogr* 31:3457–3475. doi: 10.1175/1520-  
19 0485(2001)031<3457:DWDATS>2.0.CO;2
- 20 Ballesteros E (2006) Mediterranean Coralligenous Assemblages: A Synthesis of Present Knowledge.  
21 *Oceanogr Mar Biol* 44:123–195
- 22 Barbera C, Bordehore C, Borg JA, et al (2003) Conservation and management of northeast Atlantic and  
23 Mediterranean maerl beds. *Aquat Conserv Mar Freshw Ecosyst* 13:65–76. doi: 10.1002/aqc.569
- 24 Bensch A, Gianni M, Greboval D, et al (2009) Worldwide review of bottom fisheries in the high seas. *FAO*  
25 *Fish Tech Pap* 552:145
- 26 Bentrem FW, Avera WE, Sample J (2006) Estimating Surface Sediments Using Multibeam Sonar - Acoustic  
27 Backscatter Processing for Characterization and Mapping of the Ocean Bottom. *Sea Technol* 47:37
- 28 Bernal M (2016) Management of Deep Sea Fisheries and protection of Vulnerable Marine Ecosystems in the  
29 Mediterranean Sea. In: The General Fisheries Commission for the Mediterranean, FAO - GFCM Fishery  
30 Resources Officer
- 31 Biondo M, Bartholomä A (2017) A multivariate analytical method to characterize sediment attributes from  
32 high-frequency acoustic backscatter and ground-truthing data (Jade Bay, German North Sea coast).  
33 *Cont Shelf Res* 138:65–80. doi: 10.1016/j.csr.2016.12.011
- 34 Birkett DA, Maggs C, Drig MJ (1998) An overview of dynamics and sensitivity characteristics for conservation  
35 management of marine SACs. V:1–117
- 36 Blaschke T (2010) Object based image analysis for remote sensing. *ISPRS J Photogramm Remote Sens* 65:2–  
37 16. doi: 10.1016/j.isprsjprs.2009.06.004
- 38 Bonacorsi M, Pergent-Martini C, Clabaut P, Pergent G (2012) Coralligenous “atolls”: Discovery of a new  
39 morphotype in the Western Mediterranean Sea. *Comptes Rendus - Biol* 335:668–672. doi:  
40 10.1016/j.crv.2012.10.005
- 41 Bracchi V, Savini A, Marchese F, et al (2015) Coralligenous habitat in the Mediterranean Sea: A

- 1 geomorphological description from remote data. *Ital J Geosci* 134:32–40. doi: 10.3301/IJG.2014.16
- 2 Bracchi VA, Basso D, Marchese F, et al (2017) Coralligenous morphotypes on subhorizontal substrate: A  
3 new categorization. *Cont Shelf Res* 144:10–20. doi: 10.1016/j.csr.2017.06.005
- 4 Briggs KB, Tang D, Williams KL (2002) Characterization of interface roughness of rippled sand off fort  
5 Walton Beach, Florida. *IEEE J Ocean Eng* 27:505–514. doi: 10.1109/JOE.2002.1040934
- 6 Brown CJ, Blondel P (2009) Developments in the application of multibeam sonar backscatter for seafloor  
7 habitat mapping. *Appl Acoust* 70:1242–1247. doi: 10.1016/j.apacoust.2008.08.004
- 8 Brown CJ, Smith SJ, Lawton P, Anderson JT (2011) Benthic habitat mapping: A review of progress towards  
9 improved understanding of the spatial ecology of the seafloor using acoustic techniques. *Estuar Coast  
10 Shelf Sci* 92:502–520. doi: 10.1016/j.ecss.2011.02.007
- 11 Bunting P, Clewley D, Lucas RM, Gillingham S (2014) The Remote Sensing and GIS Software Library  
12 (RSGISLib). *Comput Geosci* 62:216–226. doi: 10.1016/j.cageo.2013.08.007
- 13 Calanchi N, Colantoni P, Rossi PL, et al (1989) The Strait of Sicily continental rift systems: Physiography and  
14 petrochemistry of the submarine volcanic centres. *Mar Geol* 87:55–83. doi: 10.1016/0025-  
15 3227(89)90145-X
- 16 Chiocci FL, D’Angelo S, Romagnoli C (2004) Atlas of Submerged Depositional Terraces along the Italian  
17 Coast. Roma
- 18 Civile D, Lodolo E, Accettella D, et al (2010) The Pantelleria graben (Sicily Channel, Central Mediterranean):  
19 An example of intraplate “passive” rift. *Tectonophysics* 490:173–183. doi:  
20 10.1016/j.tecto.2010.05.008
- 21 Collier JS, Brown CJ (2005) Correlation of sidescan backscatter with grain size distribution of surficial seabed  
22 sediments. *Mar Geol* 214:431–449. doi: 10.1016/j.margeo.2004.11.011
- 23 Dartnell P, Gardner J V. (2004) Predicting seafloor facies from multibeam bathymetry and backscatter data.  
24 *Photogramm Eng Remote Sens* 70:1081–1091. doi: 10.14358/PERS.70.9.1081
- 25 De Falco G, Tonielli R, Di Martino G, et al (2010) Relationships between multibeam backscatter, sediment  
26 grain size and *Posidonia oceanica* seagrass distribution. *Cont Shelf Res* 30:1941–1950. doi:  
27 10.1016/j.csr.2010.09.006
- 28 Di Geronimo R, Giaccone G (1994) Le alghe calcaree nel detritico costiero di Lampedusa (Isole Pelagie). *Boll  
29 Accad Gioenia Sci Nat Catania* 27:5–25
- 30 Di Martino G, Innangi S, Felsani M, et al (2015) Acquisizione dati morfo-batimetrici: convenzione Isole  
31 Pelagie per il monitoraggio della prateria a *Posidonia oceanica*. CNR-SOLAR, 12 pp. [http://eprints.  
32 bice.rm.cnr.it/identificationcode6619TR201](http://eprints.bice.rm.cnr.it/identificationcode6619TR201)
- 33 Diesing M, Green SL, Stephens D, et al (2014) Mapping seabed sediments: Comparison of manual,  
34 geostatistical, object-based image analysis and machine learning approaches. *Cont Shelf Res* 84:107–  
35 119. doi: 10.1016/j.csr.2014.05.004
- 36 Ehrhold A, Hamon D, Guillaumont B (2006) The REBENT monitoring network, a spatially integrated, acoustic  
37 approach to surveying nearshore macrobenthic habitats: application to the Bay of Concarneau (South  
38 Brittany, France). *ICES J Mar Sci* 63:1604–1615. doi: 10.1016/j.icesjms.2006.06.010
- 39 Ferrini VL, Flood RD (2006) The effects of fine-scale surface roughness and grain size on 300 kHz multibeam  
40 backscatter intensity in sandy marine sedimentary environments. *Mar Geol* 228:153–172. doi:  
41 10.1016/j.margeo.2005.11.010
- 42 Folk RL (1980) *Petrologie of sedimentary rocks*. Hemphll Publ Company, Austin 170. doi:

- 1 10.1017/CBO9781107415324.004
- 2 Fonseca L, Brown C, Calder B, et al (2009) Angular range analysis of acoustic themes from Stanton Banks  
3 Ireland: A link between visual interpretation and multibeam echosounder angular signatures. *Appl*  
4 *Acoust* 70:1298–1304. doi: 10.1016/j.apacoust.2008.09.008
- 5 Fonseca L, Mayer L (2007) Remote estimation of surficial seafloor properties through the application  
6 Angular Range Analysis to multibeam sonar data. *Mar Geophys Res* 28:119–126. doi: 10.1007/s11001-  
7 007-9019-4
- 8 Francour P, Magréau JF, Mannoni AP, et al (2006) Management guide for Marine Protected Areas of the  
9 Mediterranean sea, Permanent Ecological Moorings. Univ Nice-Sophia Antip Parc Natl Port-Cros, Nice  
10 68 pp.
- 11 Giardina F, De Rubeis P (2012) Analisi della prateria a *Posidonia oceanica* (L.) Delile (Najadales,  
12 Potamogetonaceae) dell'isola di Lampedusa (AMP "Isole Pelagie", Canale di Sicilia)
- 13 Gobert S, Cambridge M, Velimirov B, et al (2006) Biology of *Posidonia*. In: Larum A, Orth R, Duarte C (eds)  
14 *Seagrasses: biology, ecology and conservation*. pp 387–408
- 15 Goff JA, Kraft BJ, Mayer LA, et al (2004) Seabed characterization on the New Jersey middle and outer shelf:  
16 correlatability and spatial variability of seafloor sediment properties. *Mar Geol* 209:147–172. doi:  
17 10.1016/j.margeo.2004.05.030
- 18 Grasso M, Lanzafame G, Rossi PL, et al (1991) Volcanic evolution of the island of Linosa, Strait of Sicily. *Geol*  
19 *Soc Italy, Mem* 47:509–525
- 20 Grasso M, Pedley HM (1985) The Pelagian Islands: a new geological interpretation from sedimentological  
21 and tectonic studies and its bearing on the evolution of the Central Mediterranean Sea (Pelagian  
22 Block). *Geol Rom* 24:13–34
- 23 Grasso M, Pedley HM (1988) Carta geologica dell'isola di Lampedusa (Isole Pelagie, Mediterraneo Centrale)  
24 1/10,000. Cartogr SELCA, Florence
- 25 Guidetti P, Milazzo M, Bussotti S, et al (2008) Italian marine reserve effectiveness: Does enforcement  
26 matter? *Biol Conserv* 141:699–709. doi: 10.1016/j.biocon.2007.12.013
- 27 Hemminga MA, Duarte CM (2000) *Seagrass ecology*, 298 pp, Online pub. Cambridge University Press
- 28 Hillman JIT, Lamarche G, Pallentin A, et al (2017) Validation of automated supervised segmentation of  
29 multibeam backscatter data from the Chatham Rise, New Zealand. *Mar Geophys Res* 0:1–23. doi:  
30 10.1007/s11001-016-9297-9
- 31 Huang Z, Siwabessy J, Nichol SL, Brooke BP (2014) Predictive mapping of seabed substrata using high-  
32 resolution multibeam sonar data: A case study from a shelf with complex geomorphology. *Mar Geol*  
33 357:37–52. doi: 10.1016/j.margeo.2014.07.012
- 34 Ierodiaconou D, Schimel ACG, Kennedy D, et al (2018) Combining pixel and object based image analysis of  
35 ultra-high resolution multibeam bathymetry and backscatter for habitat mapping in shallow marine  
36 waters. *Mar Geophys Res* 0:1–18. doi: 10.1007/s11001-017-9338-z
- 37 Innangi S, Barra M, Brando A, et al (2008) Construction of the thematic maps of the seabed along the  
38 Lucanian Tyrrhenian Coast of Maratea (PZ). *Rend Online Soc Geol Ital* 3:
- 39 Innangi S, Barra M, Di Martino G, et al (2015) Reson SeaBat 8125 backscatter data as a tool for seabed  
40 characterization (Central Mediterranean, Southern Italy): Results from different processing  
41 approaches. *Appl Acoust* 87:109–122. doi: 10.1016/j.apacoust.2014.06.014
- 42 Innangi S, Passaro S, Tonielli R, et al (2016) Seafloor mapping using high-resolution multibeam backscatter:

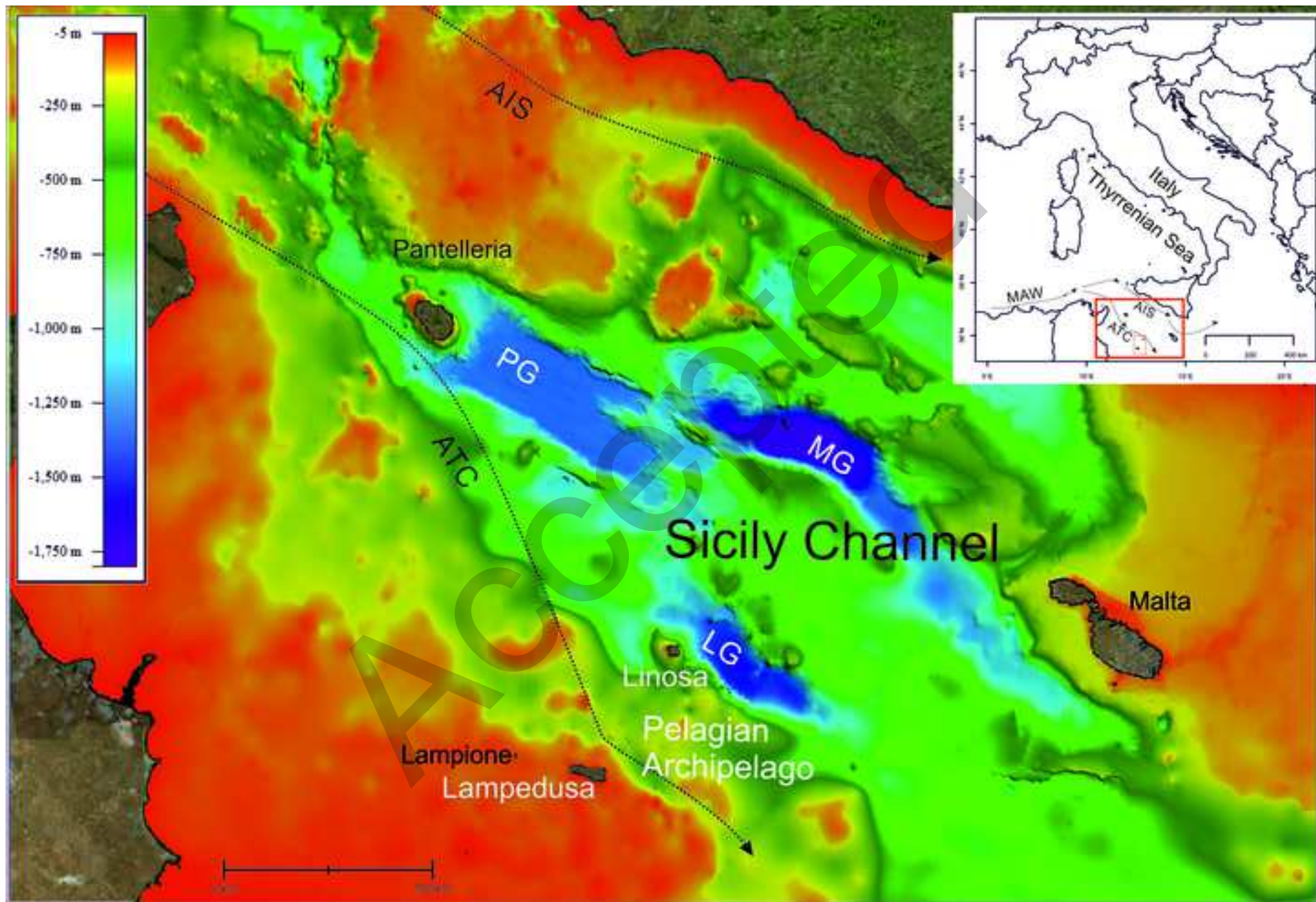
- 1 The Palinuro Seamount (Eastern Tyrrhenian Sea). *J Maps* 12:. doi: 10.1080/17445647.2015.1071719
- 2 Innangi S, Tonielli R (2017) Relazione finale della Campagna Oceanografica “Linosa.” CNR-SOLAR, 20 pp.  
3 <http://eprints.bice.rm.cnr.it/identificationcode8361TR2017>
- 4 Ismail K, Huvenne VAI, Masson DG (2015) Objective automated classification technique for marine  
5 landscape mapping in submarine canyons. *Mar Geol* 362:17–32. doi: 10.1016/j.margeo.2015.01.006
- 6 Jameson SC, Tupper MH, Ridley JM (2002) The three screen doors: Can marine “protected” areas be  
7 effective? *Mar Pollut Bull* 44:1177–1183. doi: 10.1016/S0025-326X(02)00258-8
- 8 Karoui I, Fablet R, Boucher JM, Augustin JM (2009) Seabed segmentation using optimized statistics of sonar  
9 textures. *IEEE Trans Geosci Remote Sens* 47:1621–1631. doi: 10.1109/TGRS.2008.2006362
- 10 Kostylev V, Todd B, Fader G, et al (2001) Benthic habitat mapping on the Scotian Shelf based on multibeam  
11 bathymetry, surficial geology and sea floor photographs. *Mar Ecol Prog Ser* 219:121–137
- 12 Laborel J (1987) Marine biogenic constructions in the Mediterranean. *Sci Reports Port-Cros Natl Park*  
13 13:97–126
- 14 Laborel J (1961) Le concrétionnement algal “coralligène” et son importance géomorphologique en  
15 Méditerranée. *Rec Trav Stat Mar Endoume* 23:37–60
- 16 Lacharité M, Brown CJ, Gazzola V (2017) Multisource multibeam backscatter data: developing a strategy for  
17 the production of benthic habitat maps using semi-automated seafloor classification methods. *Mar*  
18 *Geophys Res* 0:1–16. doi: 10.1007/s11001-017-9331-6
- 19 Lanti E, Lanzafame G, Rossi PL, et al (1988) Vulcanesimo e tettonica nel Canale di Sicilia: l’isola di Linosa.  
20 *Mineral Petrogr Acta* 31:69–93
- 21 Lanzafame G, Rossi PL, Tranne CA, Lanti E (1994) Carta geologica dell’isola di Linosa 1: 5000. SELCA
- 22 Le Bas T (2016) RSOBIA - A new OBIA Toolbar and Toolbox in ArcMap 10.x for Segmentation and  
23 Classification. In: Kerle N, Gerke M, Lefevre S (eds) GEOBIA 2016: Solutions and Synergies. vol.  
24 University of Twente Faculty of Geo-Information and Earth Observation, Twente, p 4
- 25 Le Bas TP, Huvenne VAI (2009) Acquisition and processing of backscatter data for habitat mapping –  
26 Comparison of multibeam and sidescan systems. *Appl Acoust* 70:1248–1257. doi:  
27 10.1016/j.apacoust.2008.07.010
- 28 Lentini F, Carbone S, Catalano S, Grasso M (1995) Principali lineamenti strutturali della Sicilia nord-  
29 orientale. *Stud Geol Camerti* 2:319–929
- 30 Li M, Zang S, Zhang B, et al (2014) A review of remote sensing image classification techniques: The role of  
31 Spatio-contextual information. *Eur J Remote Sens* 47:389–411. doi: 10.5721/EuJRS20144723
- 32 Lo Iacono C, Gràcia E, Diez S, et al (2008) Seafloor characterization and backscatter variability of the Almería  
33 Margin (Alboran Sea, SW Mediterranean) based on high-resolution acoustic data. *Mar Geol* 250:1–18.  
34 doi: 10.1016/j.margeo.2007.11.004
- 35 Lucieer V, Lamarche G (2011) Unsupervised fuzzy classification and object-based image analysis of  
36 multibeam data to map deep water substrates, Cook Strait, New Zealand. *Cont Shelf Res* 31:1236–  
37 1247. doi: 10.1016/j.csr.2011.04.016
- 38 Lucieer VL (2008) Object-oriented classification of sidescan sonar data for mapping benthic marine habitats.  
39 *Int J Remote Sens* 29:905–921. doi: 10.1080/01431160701311309
- 40 Mallace D (2012) QPS- Fledermaus Workshop- FMGeocoder Webinar. 1–49
- 41 Martin CS, Giannoulaki M, De Leo F, et al (2014) Coralligenous and maërl habitats: Predictive modelling to

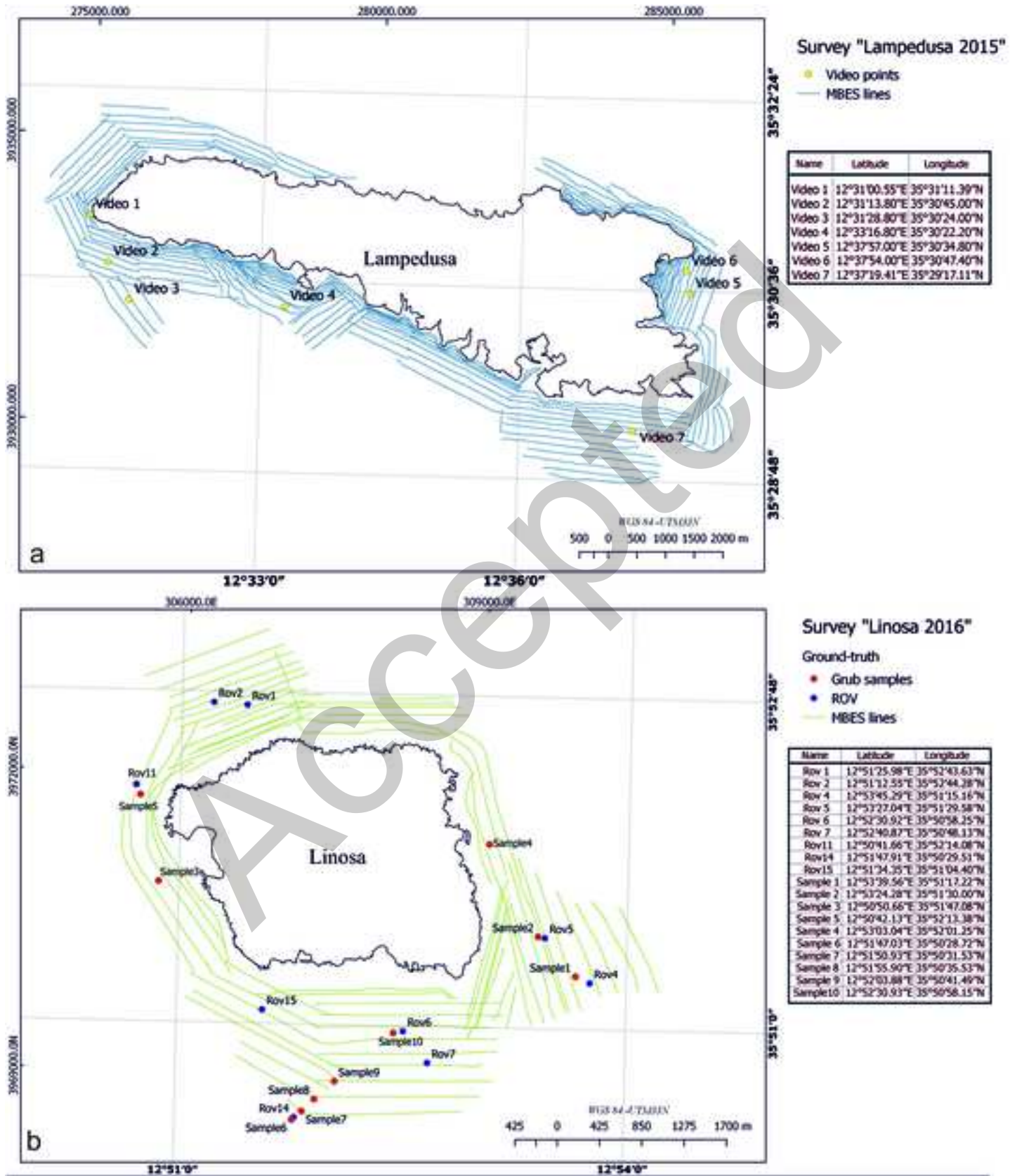
- 1 identify their spatial distributions across the Mediterranean Sea. *Sci Rep* 4:1–9. doi:  
2 10.1038/srep05073
- 3 Micallef A, Le Bas TP, Huvenne VAI, et al (2012) A multi-method approach for benthic habitat mapping of  
4 shallow coastal areas with high-resolution multibeam data. *Cont Shelf Res* 39–40:14–26. doi:  
5 10.1016/j.csr.2012.03.008
- 6 Montereale Gavazzi G, Madricardo F, Janowski L, et al (2016) Evaluation of seabed mapping methods for  
7 fine-scale classification of extremely shallow benthic habitats - Application to the Venice Lagoon, Italy.  
8 *Estuar Coast Shelf Sci* 170:45–60. doi: 10.1016/j.ecss.2015.12.014
- 9 OCEANA (2009) Developing a list of Vulnerable Marine Ecosystems. In: 40th Session of the General Fisheries  
10 Commission for the Mediterranean Mediterranean VMEs : Diverse , fragile habitats that support  
11 fisheries
- 12 Parnum I, Gavrilov A, Siwabessy P, Duncan A (2005) The effect of incident angle on statistical variation of  
13 backscatter measured using a high-frequency multibeam sonar. *Proceedings of ACOUSTICS 2005*,  
14 Busselton, Western Australia, 9-11 November, pp 433–438
- 15 Peña V, Bárbara I (2009) Distribution of the Galician maerl beds and their shape classes (Atlantic Iberian  
16 Peninsula): Proposal of areas in future conservation actions. *Cah Biol Mar* 50:353–368
- 17 Pérès JM, Picard J (1964) Nouveau manuel de bionomie benthique de la mer Méditerranée. *Recl des Trav la*  
18 *Stn Mar d'Endoume* 31:1–131
- 19 Pettijohn FJ, Potter PE, Siever R (1987) *Sand and Sandstone*, 2nd
- 20 Pieraccini M, Coppa S, De Lucia GA (2016) Beyond marine paper parks? Regulation theory to assess and  
21 address environmental non-compliance. *Aquat Conserv Mar Freshw Ecosyst*. doi: 10.1002/aqc.2632
- 22 Pomeroy RS, Watson LM, Parks JE, Cid GA (2005) How is your MPA doing? A methodology for evaluating  
23 the management effectiveness of marine protected areas. *Ocean Coast Manag* 48:485–502. doi:  
24 10.1016/j.ocecoaman.2005.05.004
- 25 Poulain P-M, Menna M, Mauri E (2012) Surface Geostrophic Circulation of the Mediterranean Sea Derived  
26 from Drifter and Satellite Altimeter Data. *J Phys Oceanogr* 42:973–990. doi: 10.1175/JPO-D-11-0159.1
- 27 QPS (ed) (2016) *Fledermaus v7.6 Manual*
- 28 Romagnoli C (2004) Submerged depositional terraces around Linosa Island (Sicily Channel). In: APAT -  
29 *Memorie descrittive della Carta Geologica D'Italia*. pp 71–74
- 30 Sartoretto S (1994) Structure et dynamique d'un nouveau type de bioconstruction à *Mesophyllum*  
31 *lichenoides* (Ellis) Lemoine (Corallinales, Rhodophyta). *Comptes rendus l'Académie des Sci Série 3, Sci*  
32 *la vie* 317:156–160
- 33 Stewart WK, Chu D, Malik S, et al (1994) Quantitative seafloor characterization using a bathymetric  
34 sidescan sonar. *IEEE J Ocean Eng* 19:599–610. doi: 10.1109/48.338396
- 35 Sutherland T, Galloway J, Loschiavo R, et al (2007) Calibration techniques and sampling resolution  
36 requirements for groundtruthing multibeam acoustic backscatter (EM3000) and QTC VIEW™  
37 classification technology. *Estuar Coast Shelf Sci* 75:447–458. doi: 10.1016/j.ecss.2007.05.045
- 38 Tonielli R, Innangi S, Budillon F, et al (2016) Distribution of *Posidonia oceanica* ( L .) Delile meadows around  
39 Lampedusa Island ( Strait of Sicily, Italy). *J Maps* 12:249–260. doi: 10.1080/17445647.2016.1195298
- 40 Truffarelli C, Belluscio A, Criscioli A, Ardizzone GD (2012) Interpretation of Sonar Images in the *Posidonia*  
41 *oceanica* cartography. *Sonograms analysis and description*. *Biol Mar Mediterr* 19:84–91
- 42 UNEP-MAP-RAC SPA (2008) Action plan for the conservation of the coralligenous and other calcareous bio-

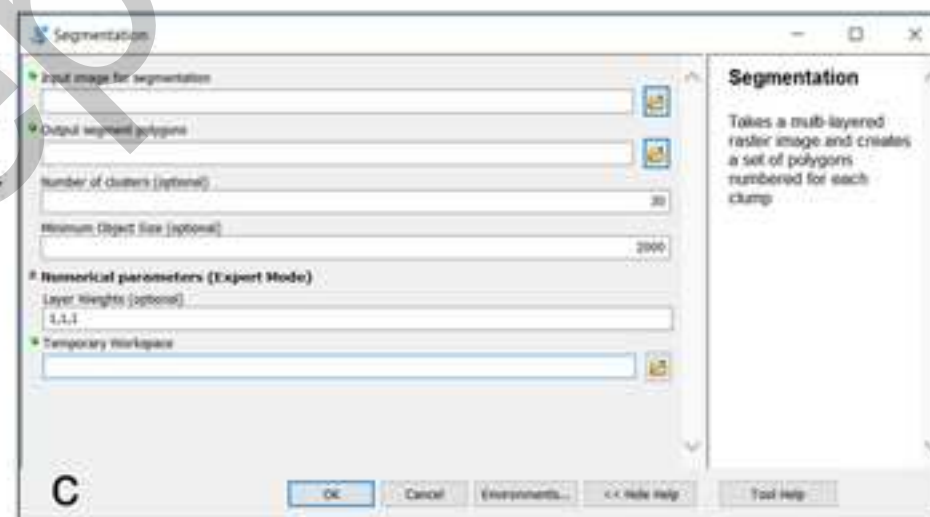
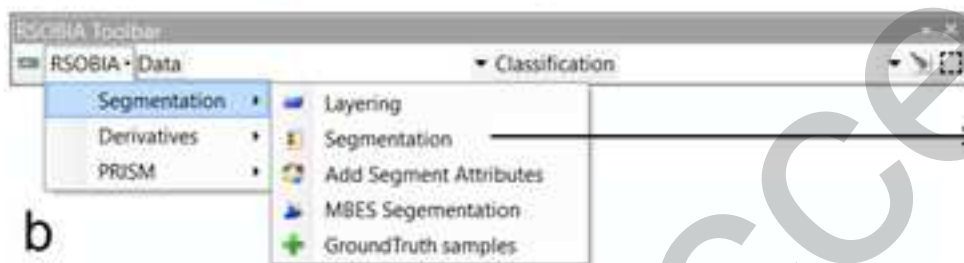
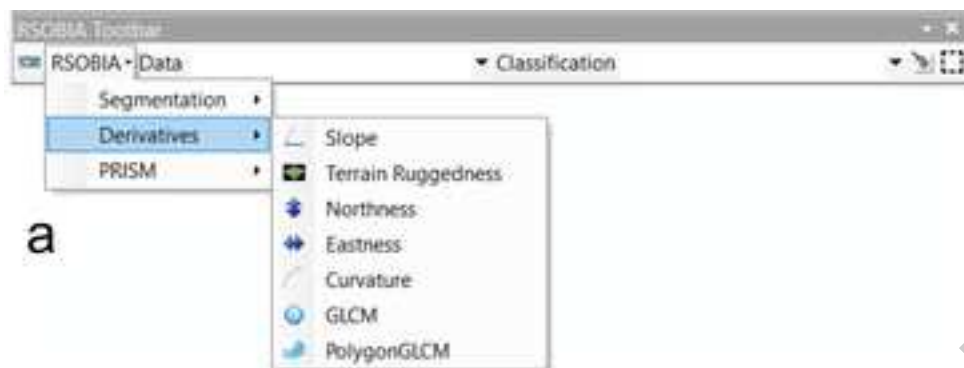
1           concretions in the Mediterranean Sea. UNEP MAP RAC-SPA publ, Tunis  
2   UNEP-MAP-RAC SPA (2015) Sicily Channel/Tunisian Plateau: Topography, circulation and their effects on  
3           biological component. UNITED NATIONS Environ Program Mediterr ACTION PLAN, Tunis  
4   Wagstaff K, Cardie C, Rogers S, Schroedl S (2001) Constrained K-means Clustering with Background  
5           Knowledge. Int Conf Mach Learn 577–584. doi: 10.1109/TPAMI.2002.1017616  
6   Wright DJ, Pendleton M, Boulware J, et al (2012) ArcGIS Benthic Terrain Modeler (BTM), v. 3.0,  
7           Environmental Systems Research Institute, NOAA Coastal Services Center, Massachusetts Office of  
8           Coastal Zone Management. esriurl com/5754

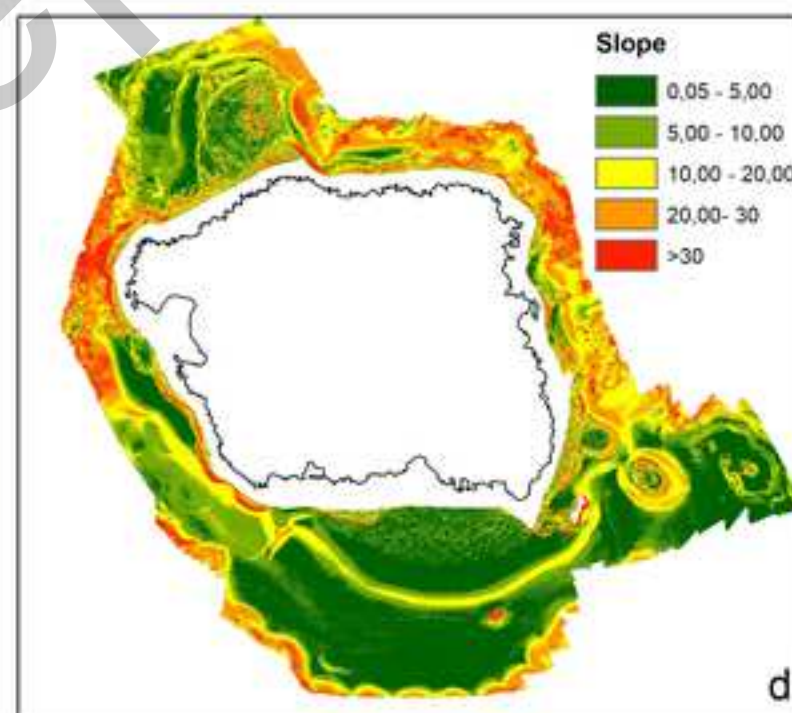
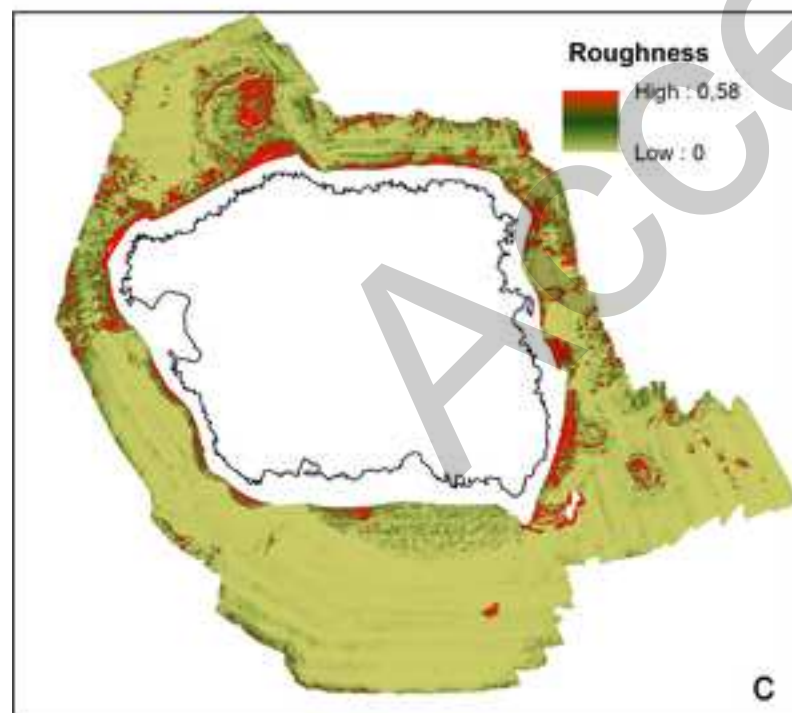
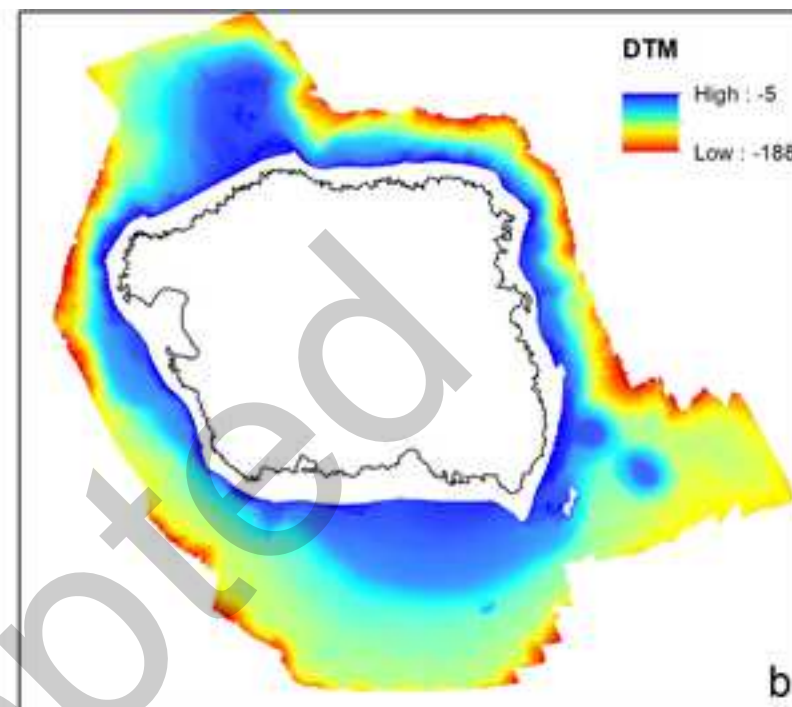
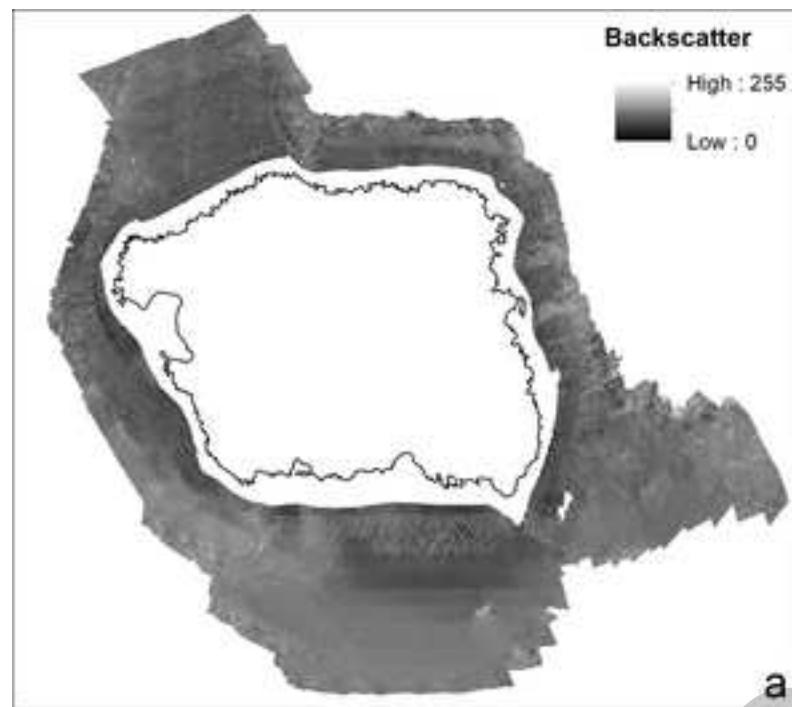
9  
10  
11  
12  
13  
14  
15  
16  
17  
18  
19  
20  
21  
22  
23  
24  
25  
26

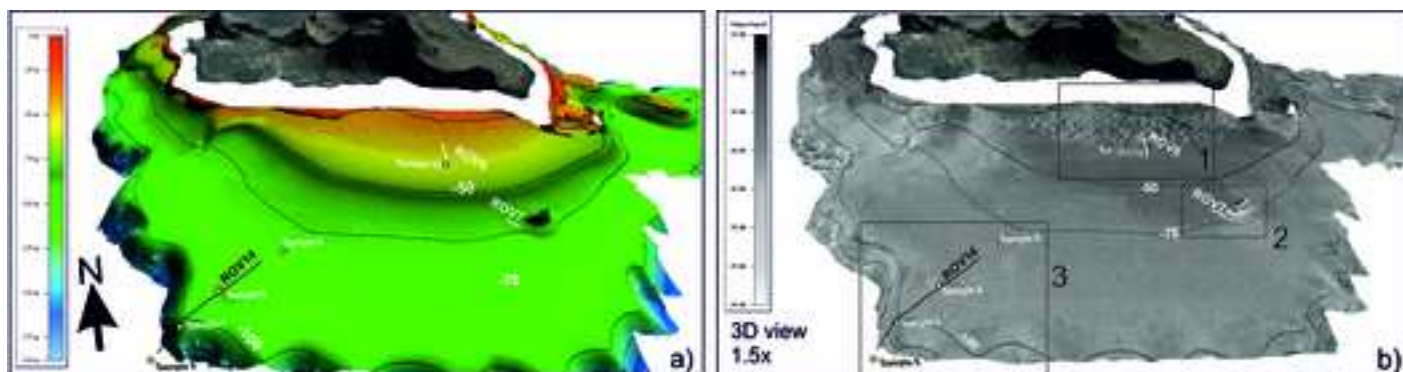
Accepted



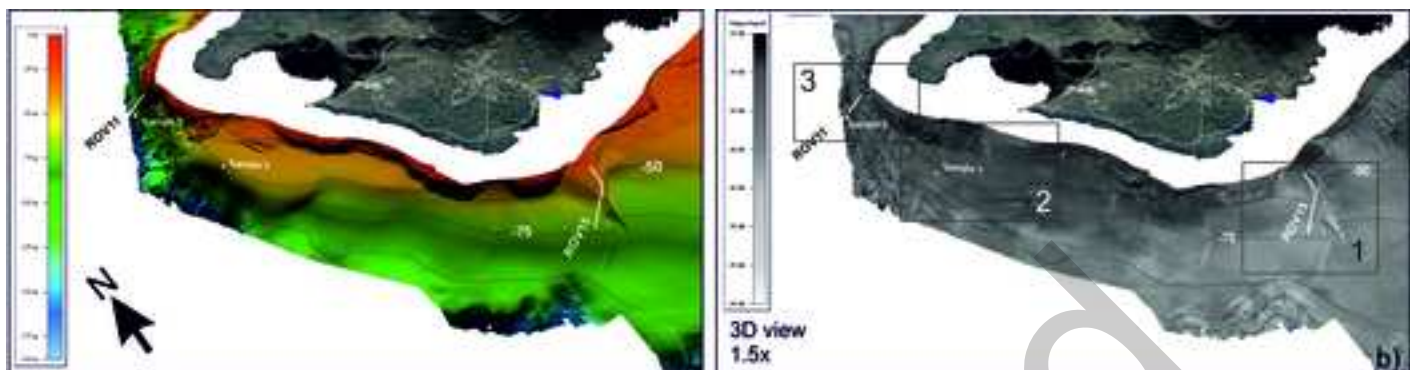


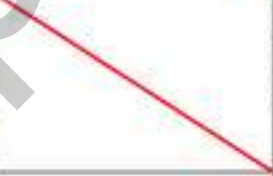
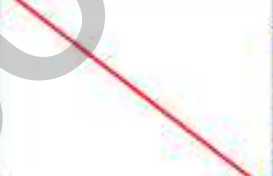
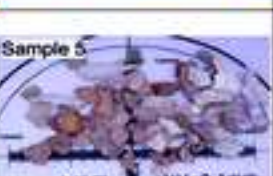
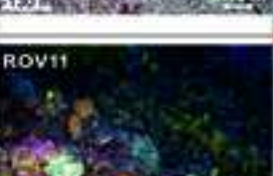


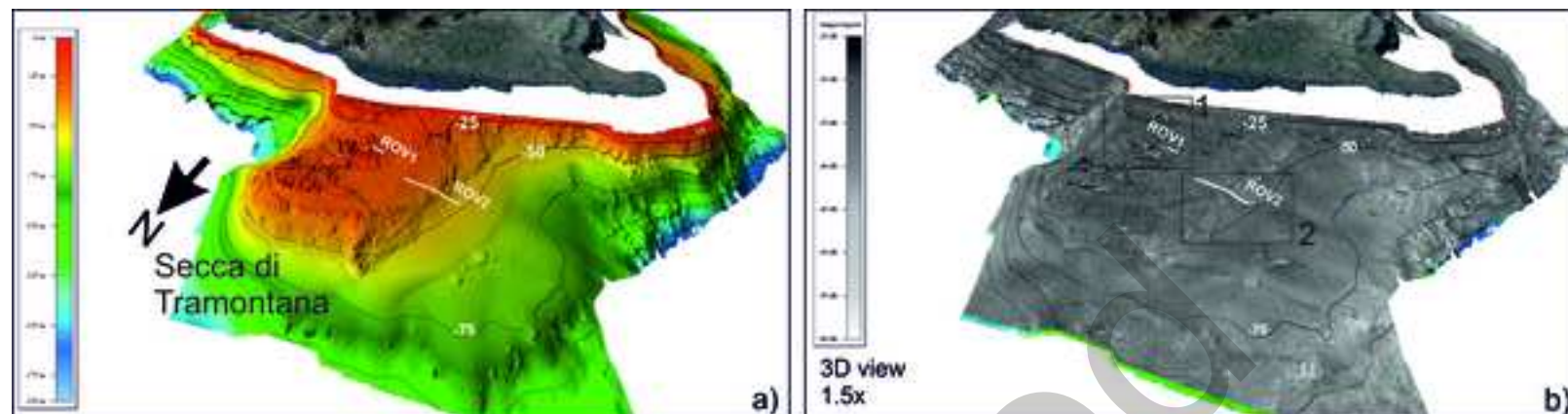




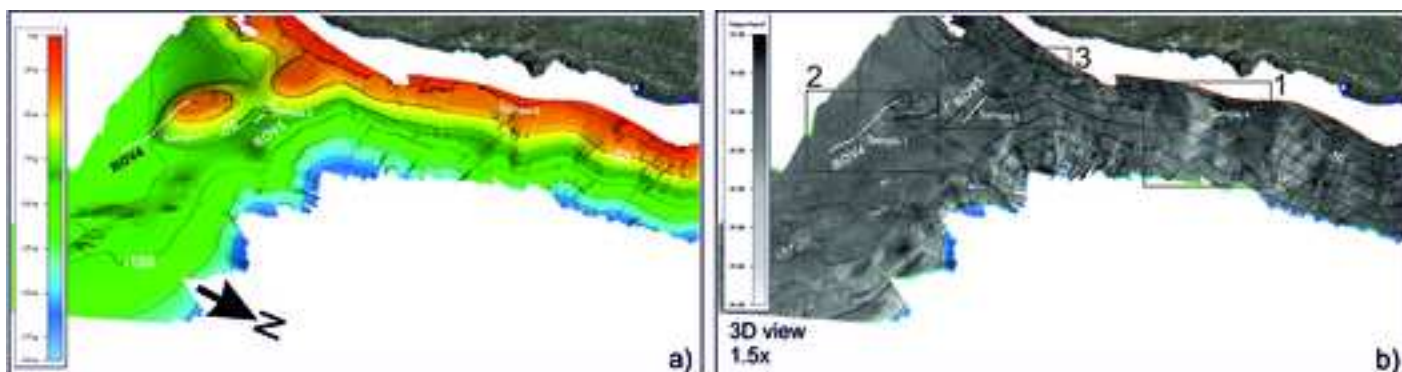
DTM	Backscatter	ROV video frame	Sample	Physical parameters	Seabed composition
Sector 1 in map					
				Intermediate backscatter pattern interrupted by elongated patches of high backscatter. Low slope ( $\sim 1.8^\circ$ )	Volcaniclastic and bioclastic coarse sand covered by dense patches of <i>P. oceanica</i> .
				Homogeneous pattern of high backscatter. Low slope ( $\sim 1.8^\circ$ )	Volcaniclastic and bioclastic coarse sand and gravel interspersed with maërl
Sector 2 in map					
				Homogeneous pattern of medium/low backscatter. Low slope ( $\sim 1.8^\circ$ )	Rhodolith and maërl beds interspersed with bioclastic coarse sand and gravel.
Sector 3 in map					
				Homogeneous pattern of medium/low backscatter. High slope ( $\sim 33^\circ$ )	Bioclastic very fine sand and gravel.
				Homogeneous pattern of medium/low backscatter. High slope ( $\sim 33^\circ$ )	Bedrock covered by dense coralligenous concretions. Bioclastic medium fine sand and gravel.
				Homogeneous pattern of medium/low backscatter. Medium/high slope ( $\sim 5^\circ - 10^\circ$ )	Bioclastic medium/coarse sand covered by dense <i>Lhytophyllum</i> and rhodolith beds
				Homogeneous pattern of medium/low backscatter. Low slope ( $\sim 0.60^\circ$ )	Bioclastic medium/coarse sand covered by dense <i>Lhytophyllum</i> and rhodolith beds

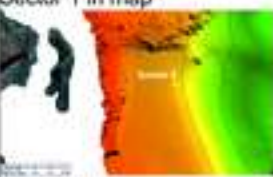
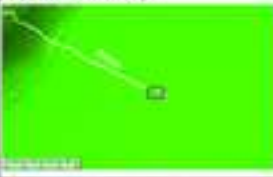
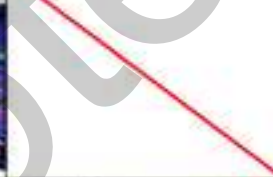
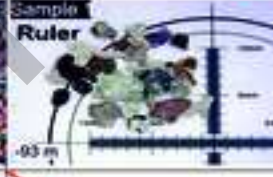
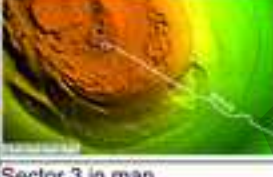
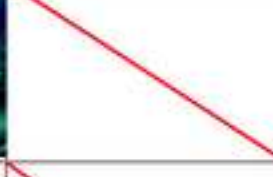
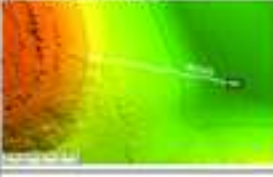
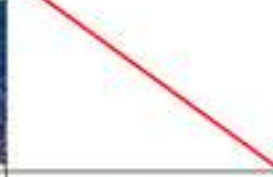
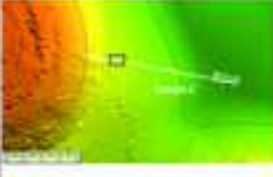
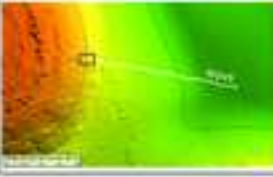
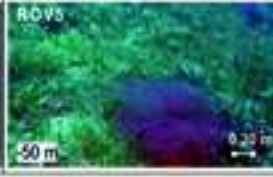
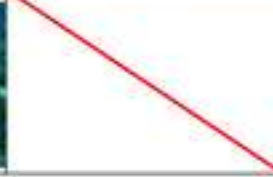


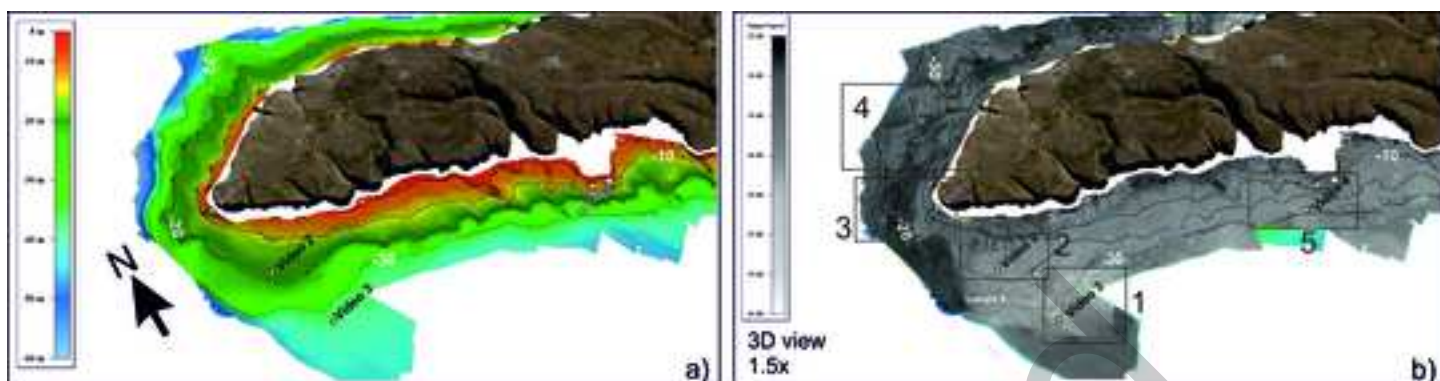
DTM	Backscatter	ROV video frame	Sample	Physical parameters	Seabed composition
Sector 1 in map 		ROV15 		Homogeneous pattern of intermediate backscatter. Intermediate slope ( $\sim 6^\circ$ )	Bioclastic and volcanoclastic medium/coarse sand
		ROV15 		Homogeneous pattern of intermediate/high backscatter. Low slope ( $\sim 1.8^\circ$ )	Volcanoclastic and bioclastic medium/coarse sand and few specimens of <i>Poceanica</i> .
Sector 2 in map 			Sample 3 	Homogeneous pattern of high backscatter. Intermediate slope ( $\sim 8^\circ$ )	Volcanoclastic medium sand.
Sector 3 in map 		ROV11 	Sample 5 	Homogeneous pattern of high backscatter. High slope ( $\sim 32^\circ$ )	Mudstone interspersed with bioclastic very coarse sand and gravel.
		ROV11 		Homogeneous pattern of high backscatter. High slope ( $\sim 32^\circ$ )	Bedrock covered by dense bioconstruction and coralligenous concretions.

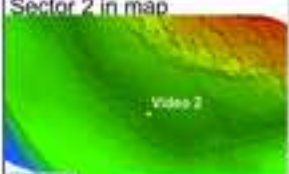
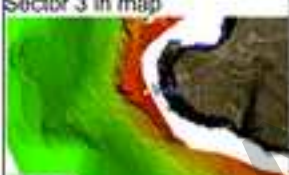
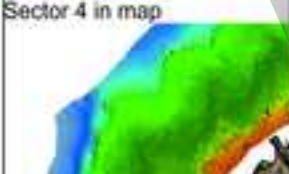
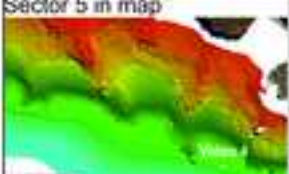


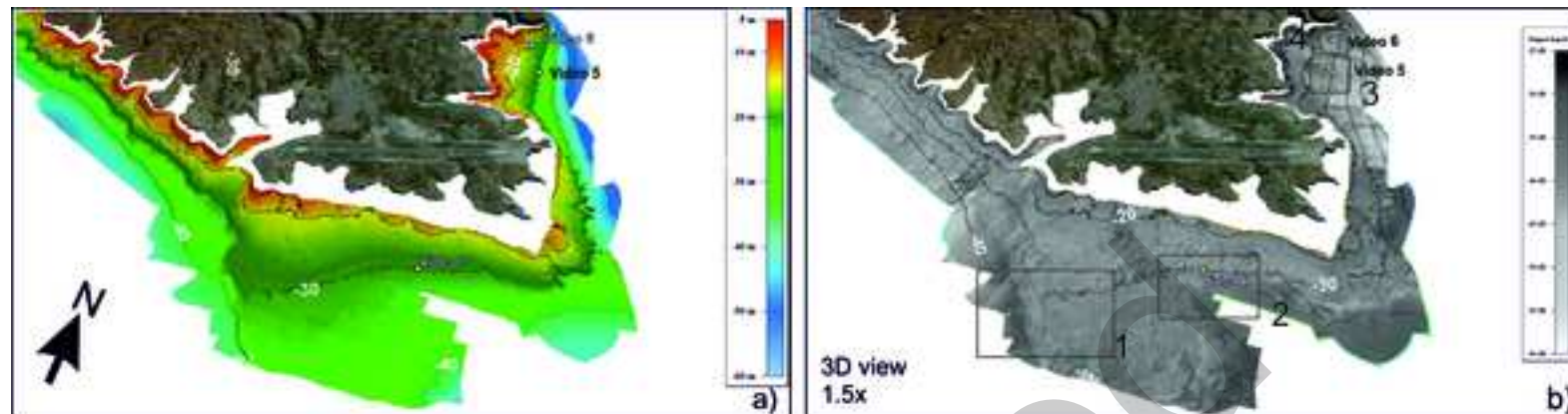
DTM	Backscatter	ROV video frame	Physical parameters	Seabed composition
Sector 1 in map				
			Homogeneous pattern of high backscatter. Low slope ( $\sim 3^\circ$ )	Bedrock covered by dense <i>P. oceanica</i> meadows
			Homogeneous pattern of high backscatter. Low slope ( $\sim 3^\circ$ )	Bedrock covered by photophilic algae and tuft of <i>P. oceanica</i>
Sector 2 in map				
			Homogeneous pattern of high backscatter. Low slope ( $\sim 2.5^\circ$ )	Bedrock covered by photophilic algae
			Homogeneous pattern of high backscatter. Intermediate slope ( $\sim 5^\circ$ )	Bedrock covered by dense <i>P. oceanica</i> meadows

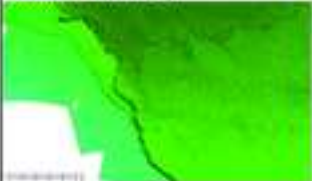
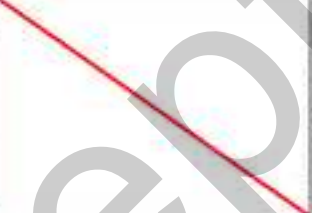
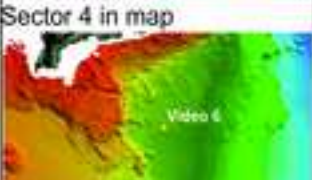


DTM	Backscatter	ROV video frame	Sample	Physical parameters	Seabed composition
Sector 1 in map 				Homogeneous pattern of low backscatter. Intermediate slope ( $\sim 6^\circ$ )	Bioclastic fine sand
Sector 2 in map 		ROV3 		Homogeneous pattern of intermediate backscatter. Low slope ( $\sim 2.5^\circ$ )	Bioclastic sand covered by dense <i>Lhytophyllum</i> and rhodolith beds
		ROV4 	Sample 1 Ruler 	Homogeneous pattern of intermediate backscatter. Intermediate slope ( $\sim 5^\circ$ )	Bioclastic and volcaniclastic coarse sand covered by dense rhodolith beds
		ROV5 		Speckled pattern of intermediate backscatter. Low slope ( $\sim 1^\circ$ )	Bedrock covered by photophilic algae
Sector 3 in map 		ROV5 		Homogeneous pattern of intermediate backscatter. Intermediate slope ( $\sim 4^\circ$ )	Bioclastic and volcaniclastic sand covered by dense rhodolith beds
		ROV5 	Sample 2 	Homogeneous pattern of intermediate backscatter. Intermediate/high slope ( $\sim 14^\circ$ )	Bioclastic and volcaniclastic coarse sand and maerl
		ROV5 		Homogeneous pattern of intermediate backscatter. High slope ( $\sim 22^\circ$ )	Bedrock covered by photophilic algae

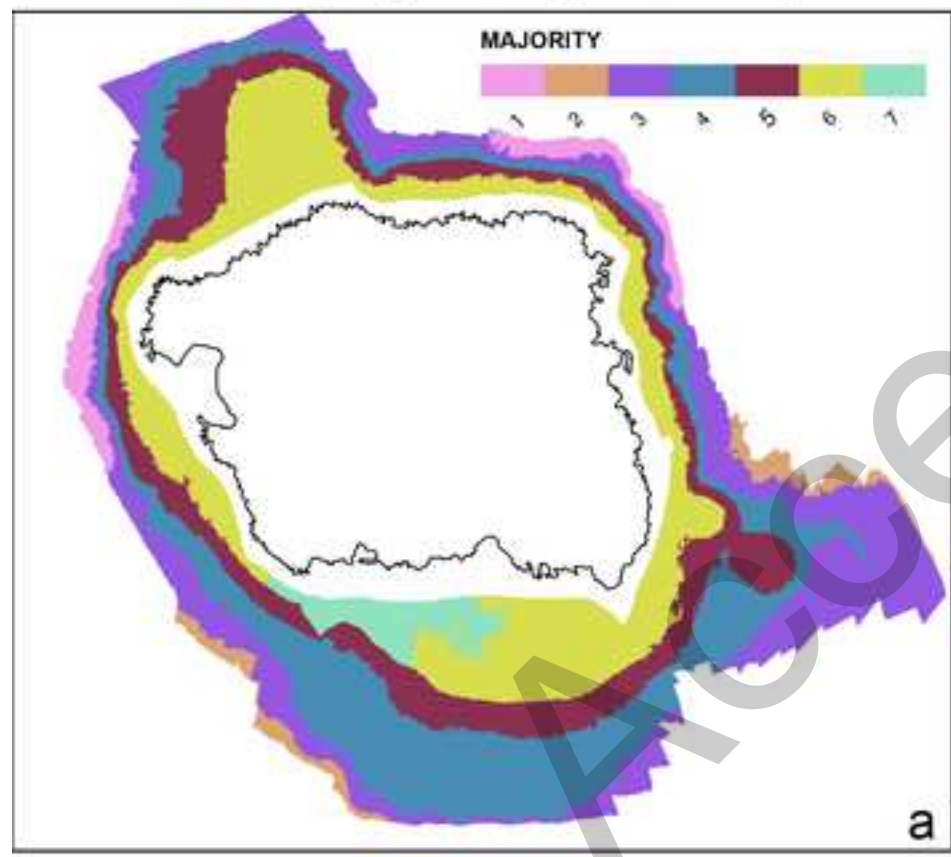


DTM	Backscatter	GoPro video frame	Physical parameters	Seabed composition
Sector 1 in map 			Dune field with NE-SW oriented crests. Low to high backscatter interrupted by an homogeneous pattern of high backscatter. Low slope ( $\sim 0.5^\circ$ )	Undulating and irregular seabed covered with soft sediments, likely composed of medium-fine sand.
Sector 2 in map 			Irregular seafloor with shortly spaced v-shaped furrows. Medium backscatter interrupted by an irregular pattern of high backscatter. To the left, homogeneous pattern of high backscatter. Low slope ( $\sim 0.5^\circ$ )	Sandy seabed covered by an irregular pattern of <i>Cymodocea nodosa</i> .
Sector 3 in map 			Rugged seabed of a terraced deposit at the foot of the submerged cliff. Speckled pattern of medium backscatter interrupted by homogeneous pattern of high backscatter. Medium slope ( $\sim 3.5^\circ$ )	Very coarse, heterogeneous materials, as well-rounded pebbles and boulders on poorly sorted gravel.
Sector 4 in map 			Below the coast, rugged seabed of a terraced deposit at the foot of the submerged cliff. Intermediate backscatter pattern interrupted by large pattern of high backscatter. Medium slope ( $\sim 2^\circ$ )	Likely substratum with coarse-grained sediment covered by an irregular pattern of <i>Posidonia oceanica</i> .
Sector 5 in map 			Homogeneous intermediate backscatter pattern interrupted by circular pattern of high backscatter. Low slope ( $\sim 0.5^\circ$ )	Superficially coarse sand to fine sand covered by dense <i>Posidonia oceanica</i> , that stops at about 38 m depth.

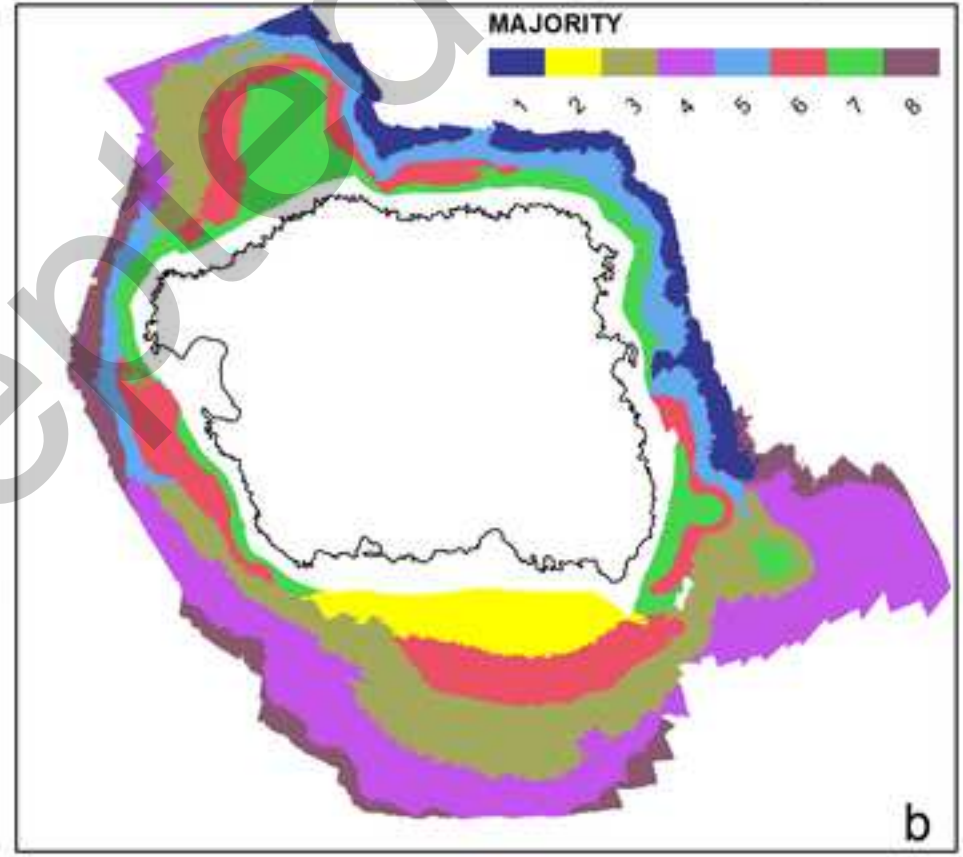


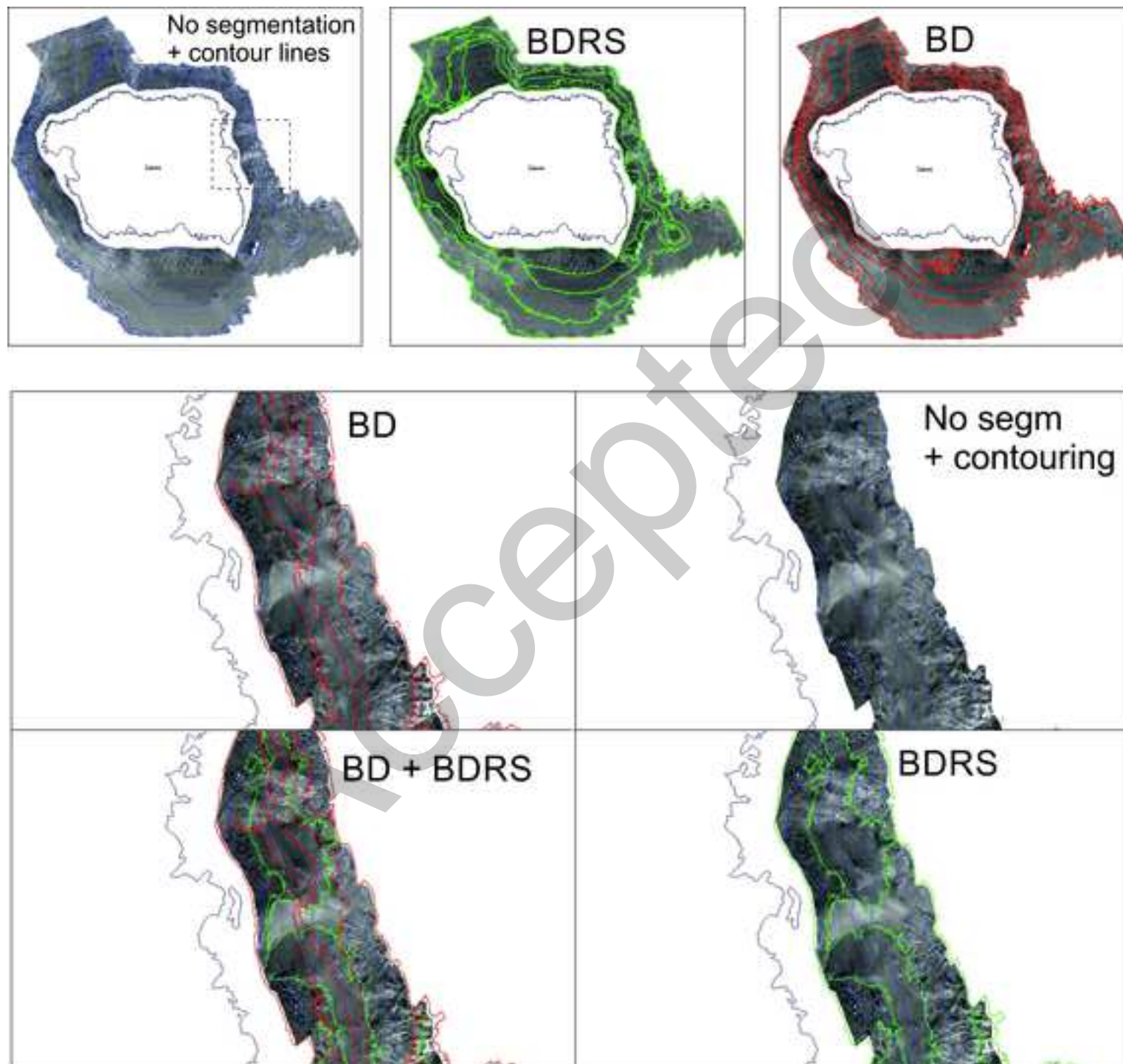
DTM	Backscatter	GoPro video frame	Physical parameters	Seabed composition
Sector 1 in map 			Rugged seafloor with intermediate backscatter pattern interrupted by elongated patches of high backscatter. Beyond 40 m depth, flat seafloor with high backscatter pattern. Low slope ( $\sim 1.8^\circ$ )	Superficially coarse sand covered by dense patches of <i>Posidonia oceanica</i> meadows.
Sector 2 in map 			Rugged seafloor with intermediate backscatter pattern interrupted by elongated patches of high backscatter. Beyond 30 m depth, flat seafloor with high backscatter pattern. Low slope ( $\sim 0.4^\circ$ )	Superficially coarse sand covered by dense patches of <i>Posidonia oceanica</i> meadows.
Sector 3 in map 			Flat seafloor with homogeneous pattern of high to intermediate backscatter. Medium slope ( $\sim 3.2^\circ$ )	Superficially coarse/medium sand.
Sector 4 in map 			Rugged seafloor with speckled pattern of intermediate backscatter. Beyond this facies, flat seafloor with alternate low and high backscatter. Low slope ( $\sim 1.5^\circ$ )	Bedrock with dense seagrass cover.

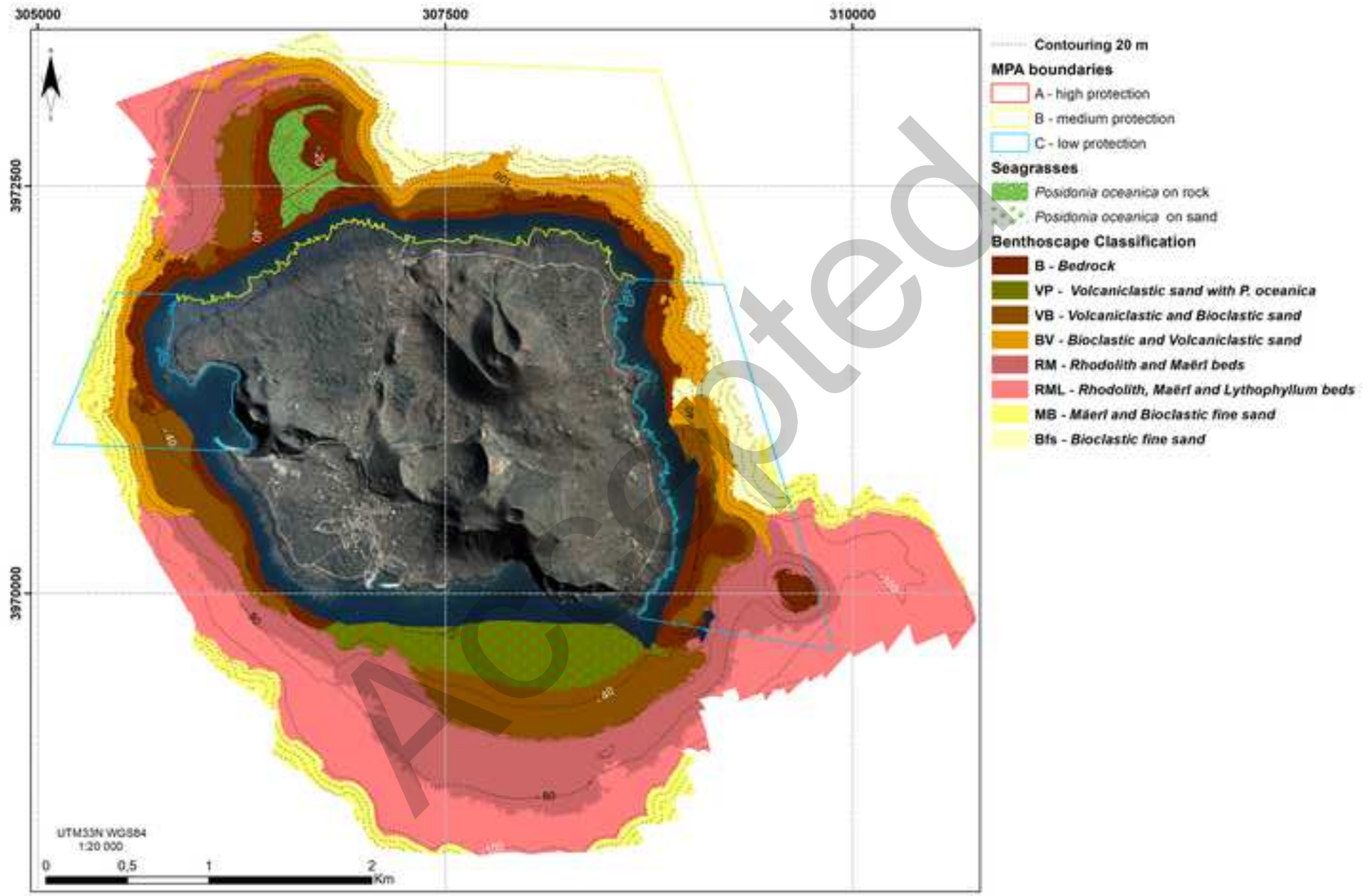
**RSOBIA *BD* Segmentation (backscatter x2)**

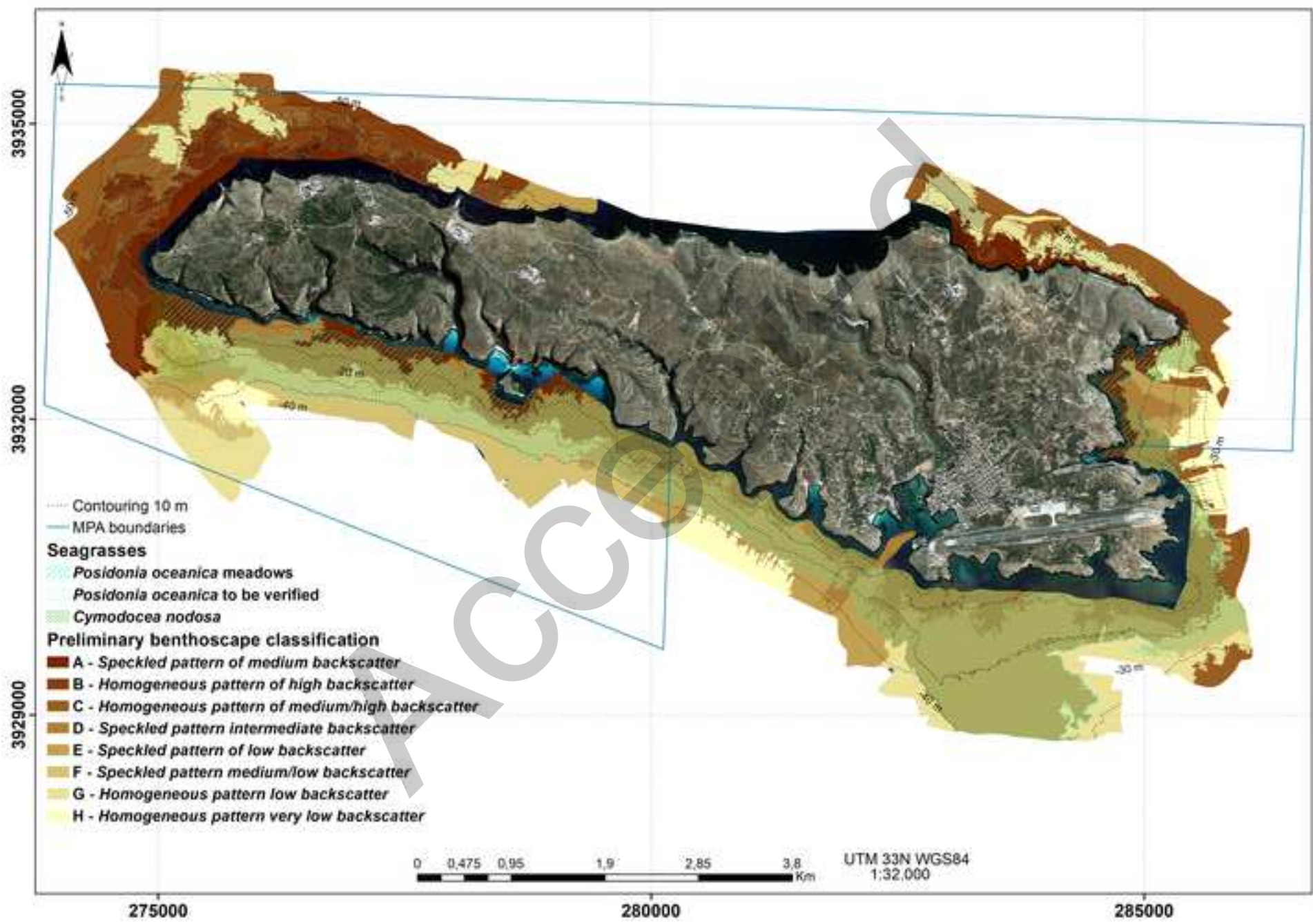


**RSOBIA *BDRS* Segmentation (backscatter x3)**

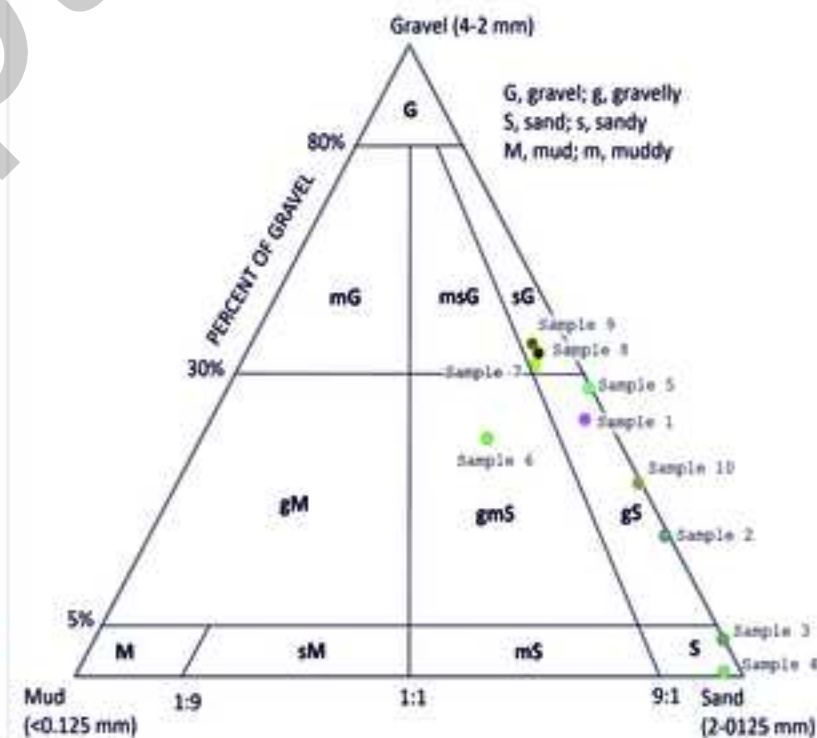
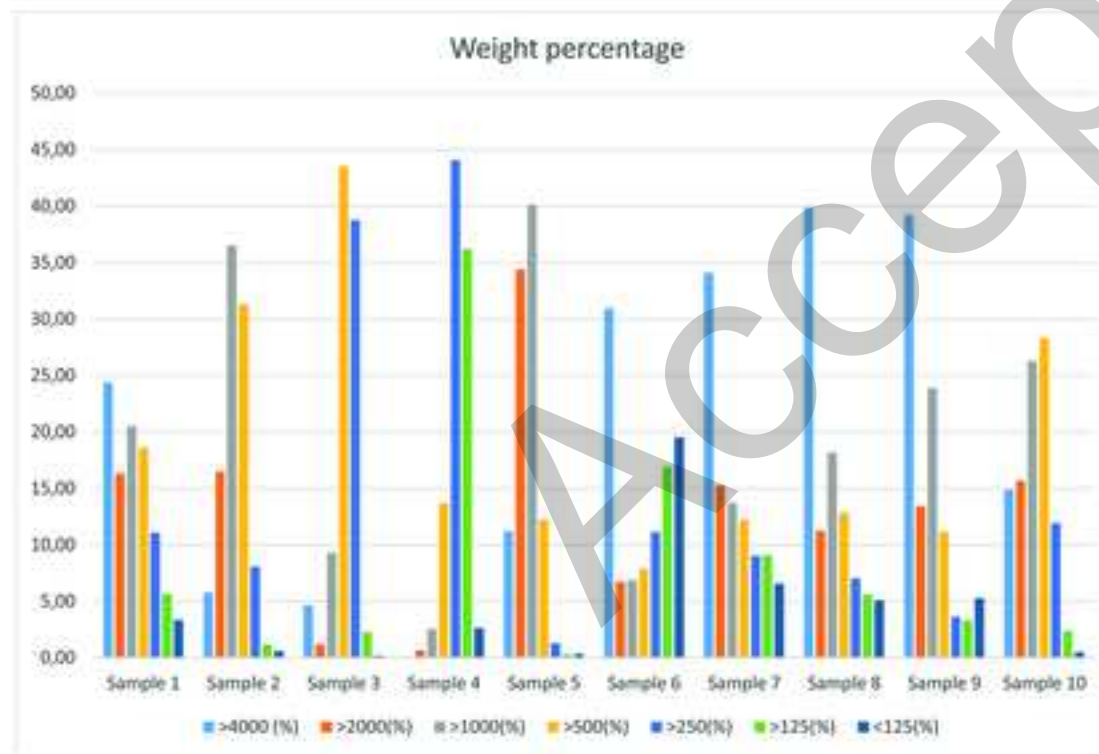




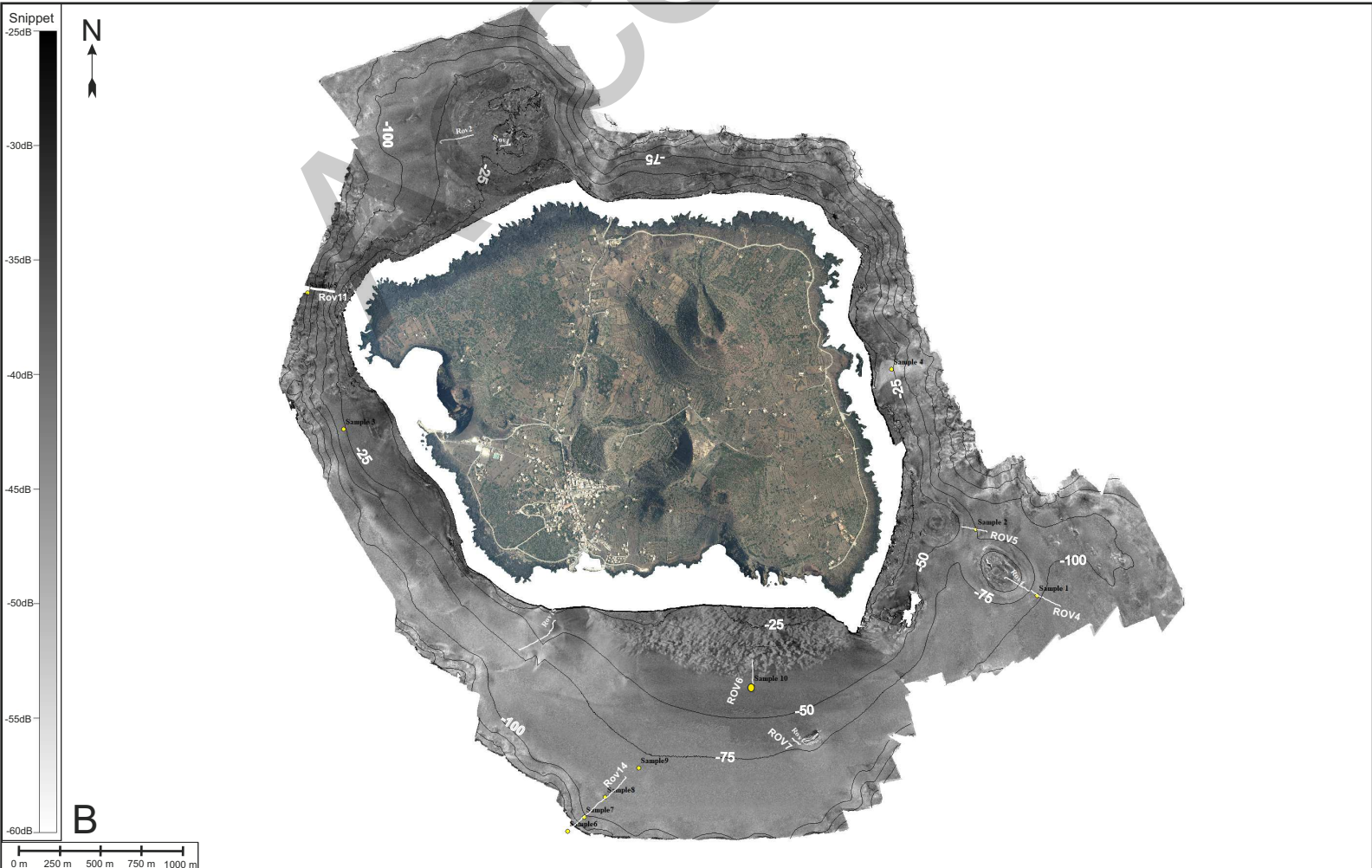
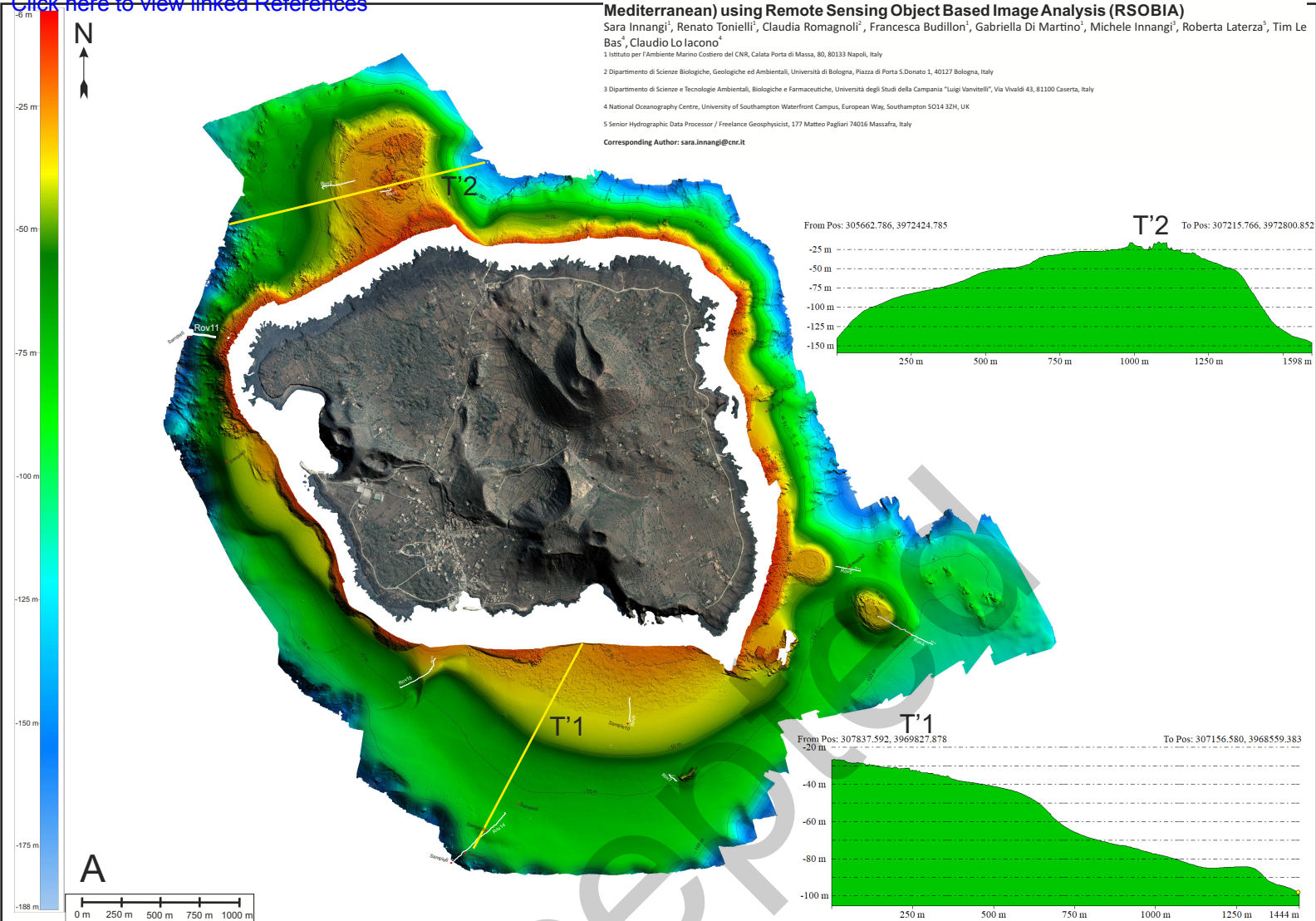




Name	Gravel (4-2mm)	Sand (2 - 0.125mm)	Silt (< 125 mm)	Folk's Classification	Wentworth's classification	Depth
Sample 1	40,73	55,91	3,36	Gravelly Sand	Coarse sand and gravel	93
Sample 2	22,29	77,11	0,60	Gravelly Sand	Coarse sand	74
Sample 3	5,88	93,93	0,19	Sand	Medium sand	54
Sample 4	0,76	96,61	2,63	Sand	Fine sand	47
Sample 5	45,68	53,99	0,33	Gravelly Sand	Very coarse sand and gravel	132
Sample 6	37,67	42,80	19,53	Gravelly muddy Sand	Very fine sand and gravel	172
Sample 7	49,36	44,06	6,58	Sandy Gravel	Medium fine sand and gravel	103
Sample 8	51,20	43,70	5,11	Sandy Gravel	Gravel and medium coarse sand	86
Sample 9	52,72	42,03	5,26	Sandy Gravel	Gravel and medium coarse sand	79
Sample 10	30,58	68,93	0,49	Gravelly Sand	Very coarse sand and gravel	40



Click here to view linked References



[Click here to view linked References](#)

**Marine Geophysical Research**

**Seabed mapping on the “Pelagie Islands” Marine Protected Area (Sicily Channel, southern Mediterranean) using Remote Sensing Object Based Image Analysis (RSOBIA)**

Sara Innangi<sup>1</sup>, Renato Tonielli<sup>2</sup>, Claudia Romagnoli<sup>3</sup>, Francesca Budillon<sup>4</sup>, Gabriella Di Martino<sup>5</sup>, Michele Innangi<sup>5</sup>, Roberta Laterza<sup>5</sup>, Tim Le Bas<sup>5</sup>, Claudio Lo Iacono<sup>4</sup>

<sup>1</sup> Istituto per l'Ambiente Marino Costiero del CNR, Calata Porta di Massa, 80, 80133 Napoli, Italy

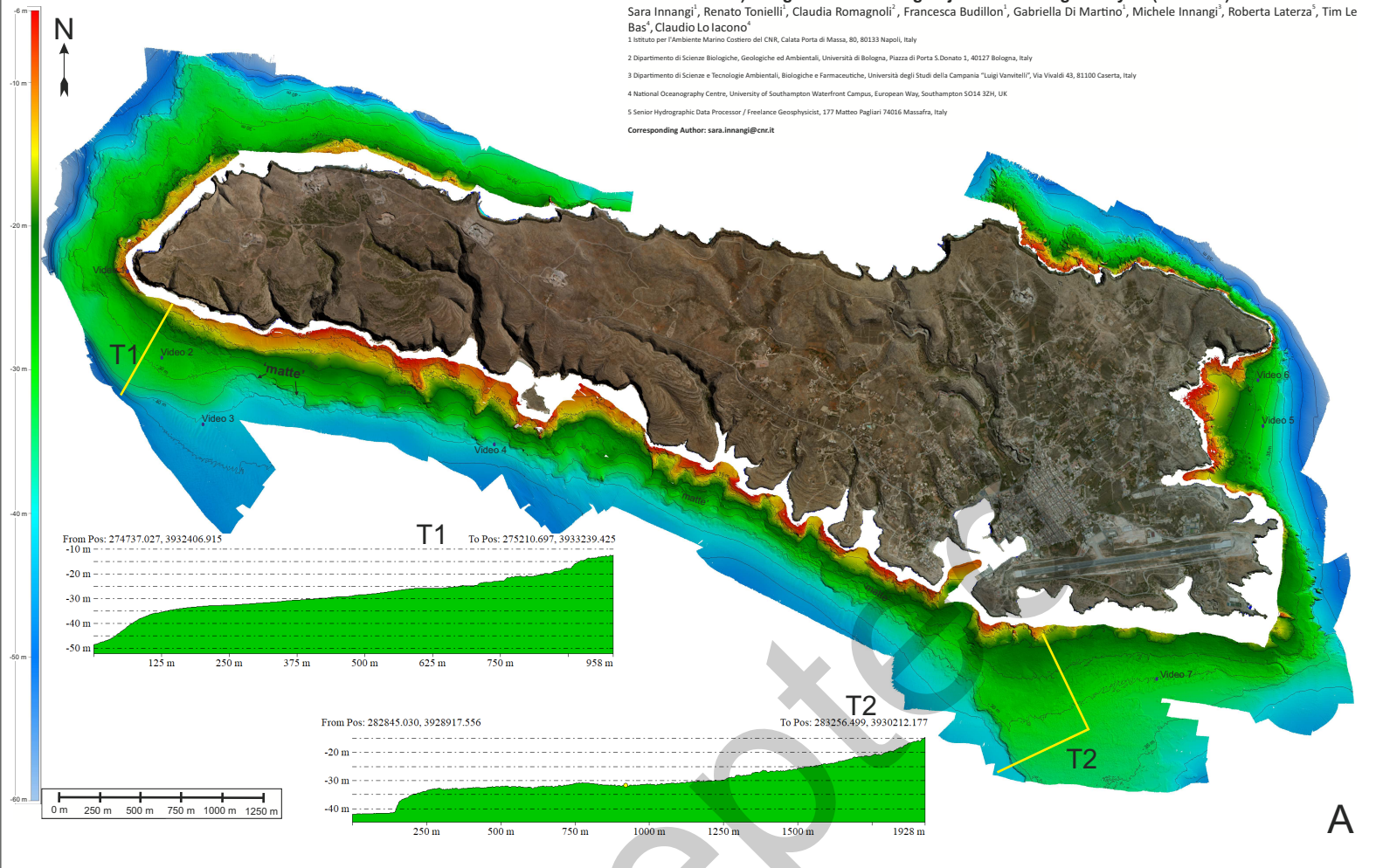
<sup>2</sup> Dipartimento di Scienze Biologiche, Geologiche ed Ambientali, Università di Bologna, Piazza di Porta S. Donato 1, 40127 Bologna, Italy

<sup>3</sup> Dipartimento di Scienze e Tecnologie Ambientali, Biologiche e Farmaceutiche, Università degli Studi della Campania “Luigi Vanvitelli”, Via Vivaldi 43, 81100 Caserta, Italy

<sup>4</sup> National Oceanography Centre, University of Southampton Waterfront Campus, European Way, Southampton SO14 3ZH, UK

<sup>5</sup> Senior Hydrographic Data Processor / Freelance Geophysicist, 177 Matteo Pagliari 74016 Massafra, Italy

Corresponding Author: sara.innangi@cnr.it



**Seabed mapping on the "Pelagie Islands" Marine Protected Area (Sicily Channel, southern Mediterranean) using Remote Sensing Object Based Image Analysis (RSOBIA)**

Sara Innangi<sup>1</sup>, Renato Tonielli<sup>2</sup>, Claudia Romagnoli<sup>2</sup>, Francesca Budillon<sup>1</sup>, Gabriella Di Martino<sup>1</sup>, Michele Innangi<sup>3</sup>, Roberta Laterza<sup>5</sup>, Tim Le Bas<sup>4</sup>, Claudio Lo Iacono<sup>4</sup>

<sup>1</sup> Istituto per l'Ambiente Marino Costiero del CNR, Calata Porta di Massa, 80, 80133 Napoli, Italy

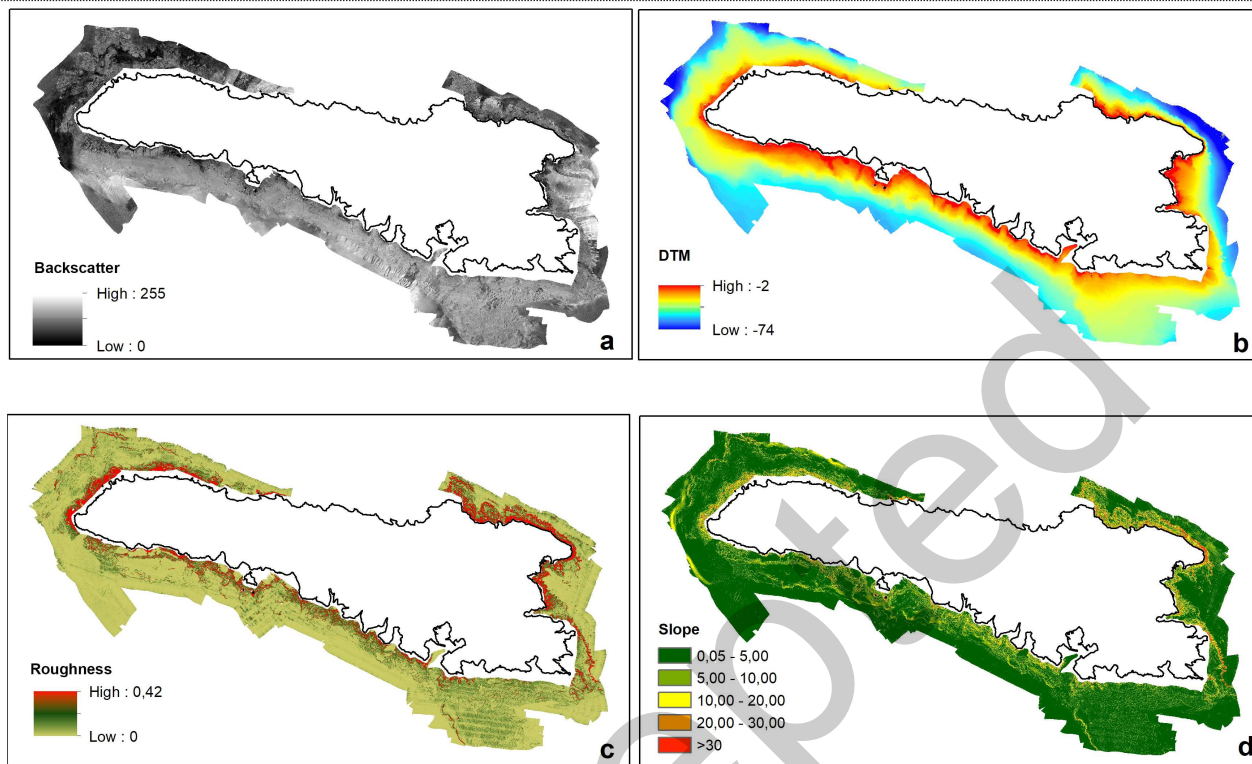
<sup>2</sup> Dipartimento di Scienze Biologiche, Geologiche ed Ambientali, Università di Bologna, Piazza di Porta S. Donato 1, 40127 Bologna, Italy

<sup>3</sup> Dipartimento di Scienze e Tecnologie Ambientali, Biologiche e Farmaceutiche, Università degli Studi della Campania "Luigi Vanvitelli", Via Vivaldi 43, 81100 Caserta, Italy

<sup>4</sup> National Oceanography Centre, University of Southampton Waterfront Campus, European Way, Southampton SO14 3ZH, UK

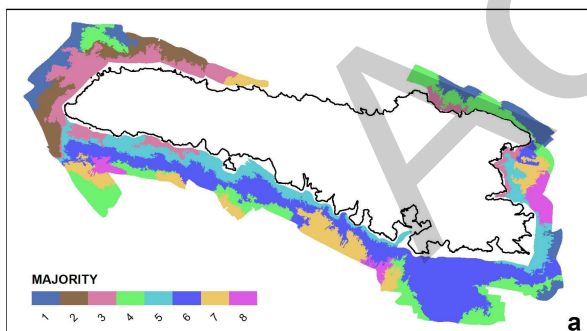
<sup>5</sup> Senior Hydrographic Data Processor / Freelance Geophysicist, 177 Matteo Pagliari 74016 Massafra, Italy

Corresponding Author: sara.innangi@cnr.it

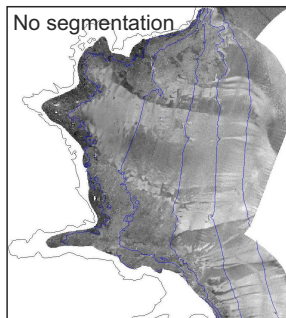
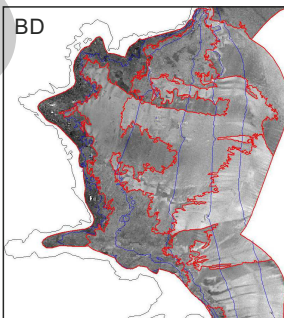
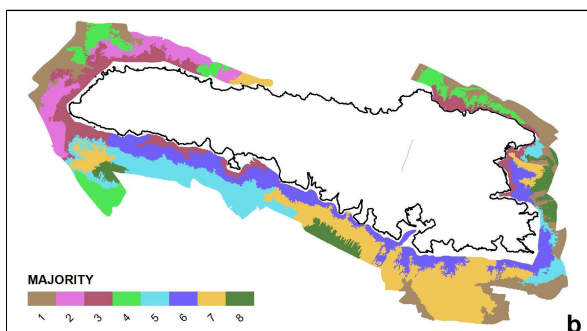


ESM3.1 - Raster images used to analyze the Lampedusa seabed with RSOBIA. a) Snippet mosaic (backscatter), with brightness values are indicated (low value corresponding high backscatter and low absorption); b) DTM image (in meters); c) the surface roughness (in dimensionless value) derived trough RSOBIA; d): the slope image (in degree) derived trough RSOBIA.

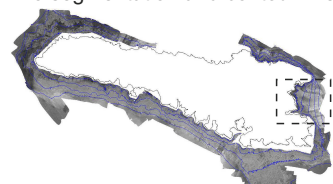
**RSOBIA BD Segmentation (backscatter x2)**



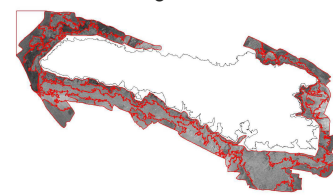
**RSOBIA BDRS Segmentation (backscatter x3)**



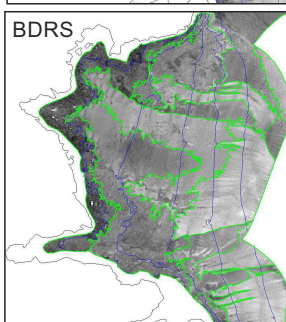
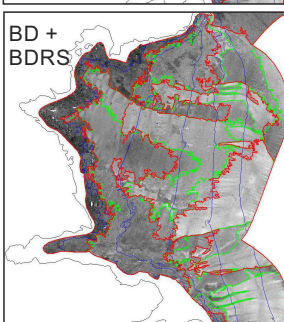
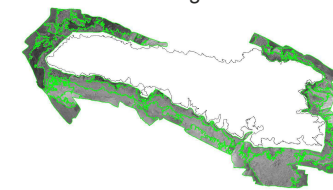
**No segmentation and contour lines**



**BD segmentation**



**BDRS segmentation**



ESM3.3 - Pairwise comparison of the two segmentations for a sector of Lampedusa. BD and BDRS segmentations were similar, and neither one looks like a counting. Nevertheless in some sector, such as in the figure, some acoustic facies are better delimited.

ESM3.2 - a) BD segmentation and b) BDRS segmentation results. The maps show the majority, the most common class of all pixels in polygon. This is the main class for interpretation.